



HAL
open science

Crossover master model of the equation-of-state for a simple fluid: critical universality

Yves Garrabos, Carole Lecoutre, Samuel Marre, Inseob Hahn

► **To cite this version:**

Yves Garrabos, Carole Lecoutre, Samuel Marre, Inseob Hahn. Crossover master model of the equation-of-state for a simple fluid: critical universality. *International Journal of Thermophysics*, 2024, 45 (6), pp.78. 10.1007/s10765-024-03359-7 . hal-04582223

HAL Id: hal-04582223

<https://hal.science/hal-04582223v1>

Submitted on 23 May 2024

HAL is a multi-disciplinary open access archive for the deposit and dissemination of scientific research documents, whether they are published or not. The documents may come from teaching and research institutions in France or abroad, or from public or private research centers.

L'archive ouverte pluridisciplinaire **HAL**, est destinée au dépôt et à la diffusion de documents scientifiques de niveau recherche, publiés ou non, émanant des établissements d'enseignement et de recherche français ou étrangers, des laboratoires publics ou privés.

Crossover Master Model of the Equation-of-State for a Simple Fluid: Critical Universality.

Yves Garrabos¹ · Carole Lecoutre¹ · Samuel Marre¹ · Inseob Hahn²

Abstract

We present a new extended parametric equation-of-state model for thermodynamic properties and the correlation length for a simple fluid near its liquid–gas critical point. The model involves 16 universal parameters to perfectly match 10 leading universal amplitudes of the asymptotic Ising-like limit of the critical-to-classical crossover functions calculated by Garrabos and Bervillier [Phys. Rev. E 74,021113 (2006)] from the massive renormalization scheme. The universal values of 8 Ising-like amplitude combinations are then matched exactly. The closure of the construction of parameters is determined after a careful analysis of the intrinsic limitation of parametric equations to describe the universal features at the first order of the confluent corrections-to-scaling. In the asymptotic mean-field limit, the crossover master model also reproduces the mean-field amplitude combinations except for the susceptibility case. The new model is compared with the crossover parametric model previously developed by Agayan et. al [Phys. Rev. E 64, 02615 (2001)]. The residuals from comparison with the mean crossover functions of Garrabos and Bervillier are reported to define the application range of the crossover master model to any simple fluid for which the generalized critical coordinates of the liquid–gas critical point are known.

Keywords Critical universality · Crossover · Simple fluids · Parametric model · Liquid-vapor · Equation-of-state

✉ Carole Lecoutre
carole.lecoutre@icmcb.cnrs.fr

Yves Garrabos
yves.garrabos@icmcb.cnrs.fr

Samuel Marre
samuel.marre@icmcb.cnrs.fr

Inseob Hahn
inseob.hahn@jpl.nasa.gov

¹ Univ. Bordeaux, CNRS, Bordeaux INP, ICMCB-UMR 5026, 33600 Pessac, France

² Jet Propulsion Laboratory, California Institute of Technology, Pasadena, CA 91109, USA

1 Introduction

Over five decades after the effective scaling analysis of thermodynamic properties in the critical region of fluids [1], the fundamental interest for developing a universal scaled form for the equation-of-state (e.o.s.) of simple fluids still is concomitant to the quest of a true asymptotic singular behavior. However, the observation of such asymptotic behavior always remains as a conundrum to the experimentalists performing measurements closer and closer to the vapor-liquid critical point [2]. Indeed, approaching the liquid-vapor critical point of a one-component fluid, i. e. a *simple* fluid with short-ranged molecular interaction, it is expected that the fluid singularities belong to the $O(1)$ universality class defined by $\{d = 3, n = 1\}$, where d is the space dimension and n is the dimension of the order parameter (OP) density [3]. In addition, the asymptotic singular properties at finite distance from T_c can be described by the classical-to-critical crossover functions calculated for the $N = 1$ -vector model of three-dimensional (3D) Ising like systems and the $O(1)$ symmetric $(\Phi^2)^2$ Field Theory (FT) framework [4]. There are two main theoretical parametric models of the classical-to-critical crossover phenomena [5–7] originated from the two main field-theoretical renormalization methods, namely the minimal-substraction renormalization (MSR) scheme of Dohm and coworkers [8–12], and the massive renormalization (MR) scheme of Bagnuls and Bervillier [7, 13–16]. However, these schemes are only applied to the primary critical path for zero value of the scaling ordering field in the homogeneous and non-homogeneous domains. The analysis of the critical fluid experiments is then limited only *asymptotically* to be conformed with the accurate estimations of the universal values of the critical exponents and amplitude combinations including the first-order of the confluent correction to scaling [17, 18]. Moreover, the theoretical analysis is strictly limited to the results obtained using a fluid cell filled at exact critical density very close to the critical temperature, in the so-called fluid *preasymptotic domain* (PAD) only characterized by two leading amplitudes and a single first-order confluent amplitude [6, 14, 17–20].

Nevertheless, still staying with these accurate measurements within the PAD (see for example [2, 21]), the actual level of knowledge of the singular features of the simple fluids seems reasonably compatible with only three adjustable free parameters in any crossover models of the e.o.s., which accurately account for the first-order confluent corrections to scaling. However, despite this now well-admitted fact that the singular one-component fluids belong to the $O(1)$ universality class, some practical difficulties still remain when the objective is to formulate the asymptotic Ising-like limit of this e.o.s.. These difficulties are unavoidable since the experimental validation of the Ising-like limit of the e.o.s. always involves measurements performed within a finite range of the phase diagram surrounding the critical point largely beyond the PAD (see for example [22] and reference therein). In such a situation, the unambiguous determination of the three Ising-like characteristic amplitudes remains problematic as the theoretical uncertainties combine with an increasing number of adjustable parameters in the e.o.s..

For instance, a phenomenological model, namely the crossover parametric model (CPM) proposed by Agayan and co-workers [5, 23, 24], introduces a complete parametric e.o.s., which needs to use at least *four* adjustable non-universal parameters. CPM results from a generic approach based on a phenomenological crossover transformation for a classical Landau expansion of the singular contribution to a free energy density [25, 26]. This generic approach was at the origin of the so-called crossover Landau model (CLM) where the van der Waals equation was used to develop the parametric form of the equation-of-state. This initial formulation by Chen et al [25, 26] was complemented by the implementation of a match-point method by Nicoll et al [27, 28]. As a consequence, CPM appears to conform with the so-called renormalization-group matching technique, while reproducing the known theoretical values for selected universal amplitudes combinations of leading amplitudes and first-order amplitudes of the confluent singularities in Wegner-like expansions [29]. Although it remains being phenomenological, this crossover model has been successfully applied to describe properties of several one-components fluids at large distances from the critical point. Furthermore, it presents the main advantage for calculating the singular thermodynamic properties in any point of the density-temperature phase surface, specially in the close vicinity of the liquid–vapor critical point in absence of experimental data. However, in spite of the essential features which evidence similar Ising-like critical behaviors from the MR and CPM crossover functions, the intrinsic small differences in universal values of the critical exponents and amplitudes combinations whatever the parametric forms used as an e.o.s. crossover model [30–32] limit the CPM interest for applications where the main objective remains the unambiguous determination of only *three* parameters that could characterize the Ising-like nature of a simple fluid in conformity with the symmetrical MR scheme.

It was previously shown [18, 33, 34] that the phenomenological master form of the MR crossover functions only involves the generalized critical point coordinates as entry data. Such phenomenological master forms provide the opportunity to define a new crossover master model (CMM), without Ising-like adjustable parameters, as suggested from Refs. [18, 22]. The only remaining differences take their origin in the choice of the selected universal values of exponents and amplitude combinations that are used to calculate the universal parameters in the crossover parametric e.o.s.. It is then our main goal of this work to determine the universal parameters of CMM analytically for the Ising-like universal exponents and amplitude ratios which are similar (or assumed similar) to the ones calculated (or expected) using the MR scheme and assuming the same level of quoted uncertainties. The present analytical determination of the CMM universal parameters provides then the exact intrinsic origin of the finite residuals from the expected MR universality. As demonstrated in the following, these residuals (of order of 3%) appear only restricted to one specific universal ratio between the first-order confluent correction amplitudes, leading to differentiate the so-called *intrinsic* and *ideal* CMM. Therefore, the Ising-like asymptotic parameter characterization of CMM results well in exact conformity with the two-scale-factor universality features calculated by the MR scheme. As in such a case already analyzed for xenon, similar analyses of the singular properties of any other simple fluid, measured at finite distance from T_c ,

should be useful to check that the single crossover parameter (noted ϑ_f , see [35]), assumed to be independent of the selected property, could characterize the confluent corrections well beyond its respective PAD. This analytical definition of the true single temperature scaling factor along the critical isochore of fluids will thus be the missing link to sustain the theoretical construction of the critical-to-classical crossover along the renormalized trajectory. In such a renormalized trajectory, only one family of corrections-to-scaling terms governed by the specific lowest value of the exponent Δ are summed into the crossover functions. In these MR crossover functions, the Ising-like asymptotic behavior within the PAD is well characterized by only *three* physical amplitudes, as previously noted. In the following CMM case, the implicit introduction of ϑ_f starts also from the asymptotic distance to the physical critical point, which defines the PAD extension where the crossover functions can be restricted to the first-order term of the confluent corrections to the scaling. Beyond the PAD, the so-called extended asymptotic domain (EAD), a similar single value of ϑ_f then defines the true validity range of the Ising-like crossover estimated along the renormalized trajectory when the non-trivial fixed point is reached. In return, it was thus generally assumed that the true initial Hamiltonian points of these actual fluids with comparable short-ranged molecular interaction lie very close to the renormalized trajectory.

The above Ising-like asymptotic characterization of the EAD can be distinguished from the characterization of the mean field limit of the critical-to-classical crossover. Until now, the introduction of the (property-dependent) Ginzburg number to rescale the mean-field temperature appeared as a convenient tool to define an order of magnitude for the limit of the mean-field crossover behavior of each property. Such a limiting criterion starts from the Gaussian fixed point of the renormalized trajectory and needs the introduction of (at *a minima*) three unknown, mean-field-like, non-universal parameters in the classical Hamiltonian (including thus a square-gradient term). Therefore, the following CMM seems better adapted to describe the simple fluid singularities since, to our knowledge, a complete crossover description from the Gaussian fixed point to the non-trivial fixed point was never observed in the subclass of simple fluids (see also below our comment related to the the crossover behavior of the effective exponents γ for the susceptibility case and β or the order parameter density case). Such a non-observation of the mean field behavior of the fluid is easily understood as the mean field approximation takes a plausible physical meaning for only a liquid very close to the triple point to satisfy the necessary high-density value of the systems. More generally, the mean-field-like van der Waals e.o.s., or any cubic e.o.s., remains only a simple convenient concept, but always incorrect on the basis of fundamental approaches developed such as, for example, extended virial forms for the dense gas properties or specific liquid theories based on the molecular dynamics simulations.

Any sophisticated crossover model of the e.o.s. incorporating more than three free parameters is beyond the scope of this work where our main central interest only concerns the physical description of the critical crossover limit, which is then expected to be universal for short-ranged molecular interactions in simple fluids. For instance, a fourth non-universal parameter can be related to the contributions of one supplementary irrelevant field. In such a case, a proper treatment for the contribution

of another confluent exponent (of value greater than Δ) in the Wegner expansions seems necessary for theoretical coherence. It can also be related to a more complex physical understanding of the microscopic nature introduced in the model, such as an additional reference to a mesoscopic length or a significant modification of the range of molecular interaction. A concomitant difficulty then appears generally in the precise experimental characterization for the expected PAD behavior of the corresponding complex physical systems, where the order parameter choice remains not unequivocal. Such a more complicated modeling strategy differs significantly from the one given initially in Ref. [14]. The latter one was mainly focused on the controlled reduction of the number of adjustable free parameters to support the experimentalists in their analyses of the measured data in simple fluids closer and closer to their gas-liquid critical point. Correlatively we note, since the 80's until today, that no theoretical progress has been made whatever the considered model to account correctly for the true physical crossover behavior in simple fluids, observed until the correlation length reaches the same order of magnitude than the range of the molecular interactions. Such an irreducible theoretical problem was illustrated for example by the crossover behavior of the effective exponents γ in Fig. 1 of Ref. [14], Fig. 1a of Ref. [18] and Fig. 2 of Ref. [22] for the susceptibility case, ν in Fig. 1b of Ref. [18] and Fig. 2 of Ref. [36] for the correlation length case, and β in Fig. 3 of Ref. [37] and Fig. 3 of Ref. [22] for the order parameter density case.

The paper is organized as follows: In Sect. 2, we recall the main features of the equations used to define the asymptotic (Ising-like and classical) limits of the parametric e.o.s. for CPM and intrinsic CMM. Section 3 provides the tables of the universal values for intrinsic CMM that can be substituted to the Tables I to IV for CPM to define the crossover thermodynamic and correlation functions. The three ideal Ising-like parameters matching between ideal CMM and MR functions is then discussed in the Sect. 4, including the correlation length case. Conclusive remarks are formulated in Section 5 just after the comparison of the MR and intrinsic CMM crossover behaviors. Additional analytical materials are given in Appendix A to demonstrate the perfect closure of CMM functions from reference to MR functions.

2 Crossover Master Model Versus Crossover Parametric model

2.1 Formulation of the Crossover Parametric Equation-of-State

In a crossover parametric equation-of-state, any point of the phase surface close to the critical point is characterized by the radial variable r , which measures the distance to the critical point, and the angular variable θ , which represents the density distance to the critical density on a contour of constant r . The corresponding parametric forms of the physical fields contain a crossover function able to represent the phenomenological classical-to-critical crossover transformation for a Landau expansion of the singular contribution of a free energy approaching the critical point. This crossover function then leads to recover the so-called Ising-like asymptotic behavior of the singular energy very close to the critical point. In such a crossover approach, the dimensionless ordering field h_1 , the dimensionless non-ordering field h_2 , and the singular part $\Delta\tilde{\Phi}_s$ of the

dimensionless thermodynamic potential Φ , can be described by parametric functional forms in terms of the variables r and θ and by appropriate scaling forms of the crossover function Y . The corresponding results are written as follows

$$h_1 = r^{\frac{3}{2}} Y^{\frac{2\beta\delta-3}{2\Delta_s}} \tilde{l}(\theta), \quad (1)$$

$$h_2 = rk(\theta), \quad (2)$$

$$\Delta\tilde{\Phi}_s = r^2 Y^{-\frac{\alpha}{\Delta_s}} \tilde{w}(\theta) + \frac{1}{2} B_{cr} r^2 (1 - b^2 \theta^2)^2, \quad (3)$$

where β , δ , and α are the critical exponents for the top shape of the coexistence curve, the antisymmetrical shape of the critical isotherm, and the singular behavior of the heat capacity at constant volume, respectively. Δ_s (in Agayan et al's notations) is identical to the lowest value of the MR critical exponent (hereafter noted Δ) for the confluent singularities (see below). $k(\theta)$, $\tilde{l}(\theta)$ and $\tilde{w}(\theta)$ are the parametric forms of present interest and B_{cr} an analytic fluctuation-induced background constant.

In the CPM, the crossover function Y is formulated to satisfy the following equation

$$1 - (1 - \bar{u})Y = \bar{u} \left(1 + \frac{\Lambda^2}{\kappa^2} \right)^{\frac{1}{2}} Y^{\frac{\nu}{\Delta_s}}, \quad (4)$$

where κ is the inverse of the dimensionless correlation length ξ^* and ν is the corresponding universal critical exponent. Equation (4) introduces the crossover parameter \bar{u} when Λ is used as a wavelength cutoff. Similarly, a parametrization of κ , as a function of r , is such as

$$\kappa^2(r) = c_t r Y^{\frac{2\nu-1}{\Delta_s}}. \quad (5)$$

The crossover function Y , like κ , are independent of θ and only linear functions of r . c_t is a dimensionless (fluid-dependent) scaling factor for the reduced temperature distance to T_c along the critical isochore. Using both Eqs. 4 and 5 defines the crossover parameter $g = \frac{(\bar{u}\Lambda)^2}{c_t}$ as a combination of the two crossover parameters \bar{u} and $\frac{\Lambda}{(c_t)^{\frac{1}{2}}}$ characterizing, respectively, the crossover shape and the crossover temperature scale of the function Y .

To describe a one-component fluid of N particles (of individual mass m_p) and total volume V using the usual intensive variables p and T associated to the mass density $\rho = N \frac{m_p}{V}$, the CMM then assumes, as in Ref. [34], that the scaling fields h_1 and h_2 can be expressed in the linear combinations of the usual reduced temperature distance

$$\Delta\tau^* = \frac{T}{T_c} - 1, \quad (6)$$

and the usual dimensionless specific chemical potential distance

$$\Delta\tilde{\mu} = \tilde{\mu} - \tilde{\mu}_c \quad (7)$$

to their respective critical values. In Eq. 7, the dimensionless form of the specific chemical potential μ_ρ reads $\tilde{\mu} = \mu_\rho \frac{\rho_c}{\rho}$. As our present construction of the CMM is mainly focused on the well-defined Ising-like critical limit of the crossover behavior calculated from the MR scheme, the energy reference $\beta_c = k_B T_c$ of the simple fluid is then proportional to its critical temperature T_c (introducing the Boltzmann constant k_B), while its volume reference is $\frac{k_B T_c}{p_c} = (\alpha_c)^d$. Moreover, to maintain the Ising-like similarity with the symmetrical $(\Phi^2)^2$ field theory, we only consider the symmetrical form of the parametric equation by fixing a zero value to the mixing parameter b_2 that measures the asymptotic singular asymmetry in the slope of the coexistence curve, i.e.,

$$b_2 = 0. \quad (8)$$

Therefore, the simplified forms of the scaling fields h_1 and h_2 write as follow

$$\begin{aligned} h_1 &= \Delta\tilde{\mu}, \\ h_2 &= \Delta\tau^*, \end{aligned} \quad (9)$$

The corresponding conjugated parameters to h_1 and h_2 are

$$\varphi_1 = - \left(\frac{\partial \Delta\tilde{\Phi}}{\partial h_1} \right)_{h_2} = \Delta\tilde{\rho}, \quad (10)$$

$$\varphi_2 = - \left(\frac{\partial \Delta\tilde{\Phi}}{\partial h_2} \right)_{h_1} = \Delta\tilde{s}, \quad (11)$$

respectively. In Eq. 10, $\Delta\tilde{\Phi} = \Delta\tilde{a} = \tilde{a} - \tilde{a}_c$ is the dimensionless difference of the Helmholtz free energy $A(T, V, N)$ versus its arbitrary critical value $A(T_c, V_c, N_c)$, with $a_H = \frac{A(T, V, N)}{V}$ ($a_{Hc} = \frac{A(T_c, V_c, N_c)}{V}$) and $\tilde{a}_H = \frac{a_H}{\rho_c}$ ($\tilde{a}_{Hc} = \frac{a_{Hc}}{\rho_c}$). Here, added subscript H avoids confusion from the correlation angular function $a(\theta, Y_1)$ introduced below. $\Delta\tilde{\rho} = \tilde{\rho} - 1$ is the dimensionless order-parameter (proportional to the density difference versus the critical density ρ_c), with $\tilde{\rho} = \frac{\rho}{\rho_c}$. In Eq. 11, $\Delta\tilde{s} = \tilde{s} - \tilde{s}_c$ is the difference between the dimensionless entropy density $\tilde{s} = \frac{S}{V} \frac{T_c}{p_c}$ versus its (arbitrary) value $\tilde{s}_c = \frac{S_c}{V} \frac{T_c}{p_c}$ at the critical point [38]. We note that the original CPM uses internal energy in place of entropy for φ_2 due to the choice of $\frac{1}{T}$ in place of T for h_2 , with significant effect on the confluent corrections for any order equal or greater than second-order, when the main objective is the comparison with MR crossover functions introducing the single characteristic crossover parameter at the first-order. Once h_1 , h_2 , $\Delta\tilde{\Phi} = \tilde{a} - \tilde{a}_c$ are defined in terms of the parametric variables r and θ , all the fluid properties can then be derived using well-known thermodynamics relations. We recall that a decoration by a tilde means a dimensionless thermodynamics quantity

for a fluid of unit mass, while the superscript * refers to a dimensionless thermodynamics quantity for a fluid particle [18]. Despite the dimensionless identity $\tilde{\Phi} = \frac{\Phi}{\rho_c} \equiv \Phi^* = \Phi \beta_c (\alpha_c)^d$ for any thermodynamic potential Φ , this distinction permits the correct account of the extensive thermodynamics nature of each fluid, especially throughout the universal combinations between dimensionless correlation properties and dimensionless thermodynamics properties, such as Q^+ or Q^+/R_C .

Following Agayan's dissertation [23], the thermodynamics extensive description is made per unit of volume V , while the volume reference for correlation length description is $v_0 \equiv (\alpha_c)^d$. In such a case, the CPM crossover behavior of the dimensionless correlation length $\xi^* = \frac{\xi}{\alpha_c}$ is specified through its relation to the dimensionless isothermal susceptibility $\tilde{\chi} = \left(\frac{\partial \rho_1}{\partial h_1}\right)_{h_2} = \left(\frac{\rho}{\rho_c}\right)^2 p_c \kappa_T$, given by the following crossover equation

$$\frac{(\xi^*)^2}{\tilde{\chi}} = Y^{-\frac{\eta\nu}{\Delta_s}} (\bar{u}\Lambda)^{-2\eta\nu} a(\theta, Y_1), \quad (12)$$

where $a(\theta, Y_1)$ is the correlation angular function that remains to define below (see Eq. 16) for the CMM case, with $Y_1(r) = \frac{1}{\Delta_s} \frac{r}{Y} \frac{dY}{dr}$. $\kappa_T = \frac{1}{\rho} \left(\frac{\partial \rho}{\partial p}\right)_T$ is the usual isothermal compressibility factor.

However for the present work, due to the fact that Y is independent of θ , we can avoid the detailed formulations of the crossover function Y , which can be found in Refs. [23, 24]. Therefore, the main concern of the next section is only focused on the formulation of new extended parametric forms of $k(\theta)$, $\tilde{l}(\theta)$, $\tilde{w}(\theta)$, $a(\theta, Y_1)$. A special attention is given on their relative effects on the estimates of the 26 amplitudes

Table 1 26 amplitudes (using Agayan's notations [23, 24]) of the crossover parametric functions considered in the present work

	Ising-like limit	1 st -order confluent corrections	Mean-field-like limit
(a) Thermodynamics [23, 24]	(7) A_0^+, A_0^- Γ_0^+, Γ_0^- B_0, D_0, Γ_0^c	(5) $A_1^+ = 2\alpha \left[1 + \frac{\Delta(3+\Delta-\alpha)}{(1-\alpha)(2-\alpha)}\right]$ $\Gamma_1^+ = 2(\gamma - 1)$ A_1^-, Γ_1^-, B_1	(6) $\overline{\Delta C_V} = \overline{A_0^-}$ $\overline{\Gamma_0^+}, \overline{\Gamma_0^-}$ $\overline{B_0}, \overline{D_0}, \overline{\Gamma_0^c}$
(b) Correlations [23]	(3) $\xi_0^+, \xi_0^-, \xi_0^c$	(2) ξ_1^+, ξ_1^-	(3) $\overline{\xi_0^+}, \overline{\xi_0^-}, \overline{\xi_0^c}$
Total: (26)	(10)	(7)	(9)

Part (a): 7 Ising-like, 5 first-order confluent corrections, and 6 mean-field-like amplitudes of thermodynamic properties; Part (b): 3 Ising-like, 2 first-order confluent correction, and 3 mean-field-like amplitudes of the correlation properties. The first-order confluent amplitudes of susceptibility (Γ_1^c) and correlation length (ξ_1^c) along the critical isotherm are not accounted for in column 3. The mean-field amplitude of the heat capacity at constant volume above T_c is fixed to zero ($A_0^+ = 0$)

of Table 1 (using Agayan's notations [23, 24]), through the use of the various auxiliary angular functions involved in the calculation of the singular behaviors of the fluid properties.

2.2 Extended Parametric Forms of the Thermodynamics and Correlation Length Angular Functions

The CMM uses the following extended analytic functions of θ :

$$k(\theta) = 1 - b^2 \theta^2, \quad (13)$$

$$\tilde{l}(\theta) = \tilde{l}_0 \theta (1 - \theta^2) (1 + d \theta^2 + e \theta^4 + f \theta^6), \quad (14)$$

$$\tilde{w}(\theta) = \tilde{m}_0 \tilde{l}_0 (w_0 + w_1 \theta^2 + w_2 \theta^4 + w_3 \theta^6 + w_4 \theta^8 + w_5 \theta^{10}), \quad (15)$$

$$\tilde{a}(\theta, Y_1) = (\tilde{m}_0)^{-\frac{5}{3}} (\tilde{l}_0)^{\frac{1}{3}} [(a_0 + a_1 \theta^2 + a_2 \theta^4) Y_1 + (a_0^* + a_1^* \theta^2 + a_2^* \theta^4) (1 - Y_1)]$$

or

$$\tilde{a}(\theta, Y_1) = (\tilde{m}_0)^{-\frac{5}{3}} (\tilde{l}_0)^{\frac{1}{3}} \left[\sum_{i=0}^2 (Y_1 a_i \theta^{2i} + (1 - Y_1) a_i^* \theta^{2i}) \right], \quad (16)$$

and the following fluctuation induced constant

$$B_{cr} = -2\tilde{m}_0 \tilde{l}_0 w_0 > 0, \quad (17)$$

where we introduce 16 *universal* parameters (b^2 , d , e , f , w_i , with $i = \{0, 5\}$, a_j and a_j^* , with $j = \{0, 2\}$) which characterize the model, while the fluid is characterized by two *non-universal* parameters \tilde{m}_0 and \tilde{l}_0 . From Eq. 12, the correlation angular function of Eq. 16 is proportional to $(\tilde{m}_0)^{-\frac{5}{3}} (\tilde{l}_0)^{\frac{1}{3}}$ as the isothermal compressibility is proportional to $\tilde{m}_0 (\tilde{l}_0)^{-1}$. Such results account for the hyperscaling universal nature of the Ising-like singular behaviors of the product $c_V \xi^3 \rightarrow Q^+$ when $\Delta \tau^* \rightarrow 0^+$, where the specific heat $c_V \propto \tilde{m}_0 \tilde{l}_0$ implies the correlation length $\xi \propto (\tilde{m}_0 \tilde{l}_0)^{-\frac{1}{3}}$. In such a Ising-like critical limit, the two parameters \tilde{m}_0 and \tilde{l}_0 are defined in the following rescaled forms

$$\tilde{m}_0 = m_0 g^{\beta - \frac{1}{2}}, \quad (18)$$

$$\tilde{l}_0 = l_0 g^{\beta \delta - \frac{3}{2}}, \quad (19)$$

of two system-dependent parameters m_0 and l_0 , which characterize the asymptotic Ising-like singular behavior of the system to be in conformity with the two-scale-factor universality (see below). Due to the singular energy form of Eq. 3, $\tilde{w}(\theta)$

introduces the dimensionless energy scale of the physical system and it is then essential to note that the product of the rescaled physical parameters is such that the ratio

$$\frac{m_0 l_0}{\tilde{m}_0 \tilde{l}_0} = g^\alpha, \quad (20)$$

appears only dependent on the physical crossover parameter g . Consequently, the universal parameter w_0 defined by the ratio

$$\frac{\tilde{w}(0)}{\tilde{m}_0 \tilde{l}_0} = w_0, \quad (21)$$

is the single universal parameter of the CMM which characterizes the dimensionless energy of the universal model of dimensionless volume unity *above* T_c . From Eq. 17, we obtain

$$\mathfrak{Z}_{B_{cr}} = \frac{B_{cr}}{\tilde{m}_0 \tilde{l}_0} = -2w_0, \quad (22)$$

introducing the notation of the quantities independent of the system-dependent parameters m_0 and l_0 (see below Eqs. 30, 31 and 32). Moreover, anticipating the following construction of the intrinsic CMM, we introduce four additional universal sums of the w_i , with $i = \{0, 5\}$, and b^2 parameters and one additional universal sum of the d, e, f parameters:

$$\Sigma_0 = \frac{\tilde{w}(1)}{\tilde{m}_0 \tilde{l}_0} = \sum_{i=0}^{i=5} w_i, \quad (23)$$

$$\Sigma_1 = \frac{\tilde{w}'(1)}{\tilde{m}_0 \tilde{l}_0} = 2 \sum_{i=0}^{i=5} i w_i, \quad (24)$$

$$\Sigma_2 = \frac{\tilde{w}''(1)}{\tilde{m}_0 \tilde{l}_0} = 2 \sum_{i=0}^{i=5} i(2i-1) w_i, \quad (25)$$

$$S_0 = \frac{\tilde{w}(\frac{1}{b^2})}{\tilde{m}_0 \tilde{l}_0} = \sum_{i=0}^{i=5} w_i \left(\frac{1}{b^2}\right)^i, \quad (26)$$

$$L_0 = \frac{\Delta \tilde{l}_0}{\tilde{l}_0} = \frac{\tilde{l}(1)}{\tilde{l}_0} = 1 + d + e + f. \quad (27)$$

The latter sum of Eq. 27 is a convenient measure of the relative modification of Eq. 14 for the CMM case versus the CPM case where $d = e = f = 0$. To complement the above energy characterization above T_c , we note that the universal sum

Σ_0 defined by Eq. 23 is the single universal sum of CMM, which characterizes the dimensionless energy of the universal model of dimensionless volume unity *below* T_c . Therefore, we expect $w_0 \propto \Sigma_0$, as demonstrated in next Section. As a noticeable practical interest, Σ_0 can be used in Appendix as a single scaling factor to rescale all the CMM universal quantities w_i and the related angular functions.

The above Eqs. 13 to 17 need to define 10 universal parameters (b^2, d, e, f , and w_i , with $i = \{0, 5\}$) for the modelling of the thermodynamic properties and 6 additional parameters (a_j and a_j^\star , with $j = \{0, 2\}$) for the modelling of the correlation lengths of each fluid. As in the Agayan's notation for the correlation length cases, superscript \star in Eq. 16 distinguishes the 3 mean-field-like parameters from the 3 Ising-like parameters.

We note that $a_2 = a_2^\star = 0$ in the Agayan's CPM formulation (see Eq. 5.177 of the Agayan dissertation). Moreover, in this initial formulation of the CPM, the thermodynamic parameters d, e, f , and w_5 are equal to zero, while $w_0 = -1$ is a fixed parameter. The remaining 5 parameters b^2 and w_i ($i = \{1, 4\}$) were chosen such that the asymptotic amplitude ratios and combinations, agree, as close as possible, with a restricted number of theoretical predictions of the universal asymptotic features of 3D Ising-like systems belonging to the $\{d = 3, n = 1\}$ universality class [16, 31]. Nevertheless, a careful analysis of Ref. [24] shows that, selecting $b^2 = 1.691047$ and $w_0 = -1$, fixes unequivocally all the four remaining values of w_i ($i = \{1, 4\}$) (see Table IV of Ref. [24]), through 4 values of 4 universal combinations and ratios (see 4 upper lines of their Table II) between 6 leading thermodynamic amplitudes $A_0^+, A_0^-, \Gamma_0^+, \Gamma_0^-, B_0$, and D_0 (see Eqs. (2.18) to (2.21) in Ref. [24]). For example, CPM value $\Sigma_0 = -0.94970813$ (see Table 4) is well in agreement with the universal ratio $\frac{A_0^+}{A_0^-} = (b^2 - 1)^{2-\alpha} \frac{w_0}{\Sigma_0} = 0.52369$ (see below Eq. 38). As a consequence, among the 6 universal asymptotic parameters b^2 and w_i , only two, namely b^2 and w_0 , are independent in order to satisfy the two-scale-factor universality in the CPM case. The independence of b^2 is trivial as $k(1) = 1 - b^2$ is a quantity independent of the physical system, while the independence of w_0 as dimensionless energy reference of the model was discussed just above (see Eq. 21).

In a similar fashion, b^2 and w_0 are also independent in our present intrinsic (or ideal) CMM case and the intrinsic features of the parametric models [39] can be easily explained through some irreducible characteristic features of the angular functions, anticipating a more detailed discussion given in Appendix.

Indeed, the crossover forms of the CMM can be characterized from a crossover approach based on the Wegner-like expansions where are distinguished the two limiting asymptotic behaviors for any physical property P^l along the thermodynamic line labeled by the superscript l . For instance, along the critical isochore where $l = +, -$ for $T > T_c$ and $T < T_c$, the Ising-like critical limit $|\Delta\tau^*| \rightarrow 0$ approaching the liquid-vapor critical point and the mean-field-like classical limit $|\Delta\tau^*| \gg 1$ at large distance from T_c are well characterized by the respective following power law equations,

Table 2 MR (or CMM), CPM, and MF values of the critical exponents, where here α and γ are selected as two independent leading exponents, and ω as the characteristic exponent of the first-order confluent corrections

Ref.	Universal exponents			MF
	MR or CMM	CPM		
	[7]	[24]		
α	0.1088375	0.110	α_{mf}	0
γ	1.2395935	1.239	γ_{mf}	1
$\beta = \frac{1}{2}(d\nu - \gamma)$	0.325785	0.3255	β_{mf}	$\frac{1}{2}$
$\delta = \frac{d\nu + \gamma}{d\nu - \gamma}$	4.80495	4.80645	δ_{mf}	3
$\nu = \frac{2-\alpha}{d}$	0.6303875	0.630	ν_{mf}	$\frac{1}{2}$
$\eta = 2 - \frac{\gamma}{\nu}$	0.03360076	0.033333	η_{mf}	0
ω	0, 79616			
$\Delta = \omega\nu$	0.50189	0.52	Δ_{mf}	$\frac{1}{2}$

The column 2 must be used for CMM on place of Table I of Ref. [24] for CPM (here recalled in column 3)

$$P_{\text{Ising}}^l(|\Delta\tau^*| \rightarrow 0) = P_0^l |\Delta\tau^*|^{-\pi_P} [1 + P_1^l |\Delta\tau^*|^\Delta], \quad (28)$$

$$P_{\text{mf}}^l(|\Delta\tau^*| \gg 1) = \overline{P}_0^l |\Delta\tau^*|^{-\pi_{P,\text{mf}}}, \quad (29)$$

In such limiting descriptions, the non-universal character of the fluid enters in the Ising-like leading amplitude P_0^l , the first-order confluent correction amplitude P_1^l , and the mean-field leading amplitude \overline{P}_0^l . π_P , Δ , and $\pi_{P,\text{mf}}$ are the related universal critical exponents considered in present work (see Table 2). Accounting for the CMM results given in Appendix A (see also Table III and Eqs. (4.45) to (4.49) in Ref. [24]), the non-universal amplitudes of Eqs. 28 and 29 must be then rewritten in the following universal scaling ratios

$$\frac{P_0^l}{f_{P,\text{Ising}}^l(m_0, l_0)} = \mathfrak{Z}_P^l, \quad (30)$$

$$\frac{P_1^l}{f_{P,\text{CC}}^l(\Delta, g, \bar{u})} = \mathfrak{Z}_P^{1,l}, \quad (31)$$

$$\frac{\overline{P}_0^l}{f_{P,\text{mf}}^l(\tilde{m}_0, \tilde{l}_0)} = \overline{\mathfrak{Z}}_P^l, \quad (32)$$

where the non-universal character of the fluid is now contained, on the one hand, in the leading terms $f_{P,\text{Ising}}^l(m_0, l_0)$ and $f_{P,\text{mf}}^l(\tilde{m}_0, \tilde{l}_0)$, which express the (Ising-like or

mean-field-like) property P^l in units of $\{m_0, l_0\}$ or $\{\tilde{m}_0, \tilde{l}_0\}$ and on the other, in the confluent term $f_{P,CC}^l(\Delta, g, \bar{u}) = \frac{Y_{10}}{2\Delta} = g^{-\Delta}(1 - \bar{u})$, which expresses the common scaling factor characterizing the contribution of the single non-relevant field (for the Y_{10} formulation, see Eq. 4.35 in Ref [24]). Therefore, the 26 prefactors \mathfrak{Z}_P^l , $\mathfrak{Z}_P^{1,l}$, and \mathfrak{Z}_P^l are universal constants related to the 16 universal parameters of the CMM through the auxiliary angular (asymptotic, correction-to-scaling, and classical) functions given in Ref. [24]. However, among the 26 selected prefactors, the following 6 prefactors related to the Ising-like singular behaviors (including the first-order confluent correction-to-scaling) of the specific heat above and below T_c and the isothermal compressibility above T_c show remarkable links to the Ising exponents α , γ , and Δ and to the b^2 , w_0 , Σ_0 and w_1 parameters, i.e.,

$$\mathfrak{Z}_C^{1,+} = [2\alpha + 2\Delta q_{2,1}(0)] = 2\alpha \left[1 + \frac{\Delta(3 + \Delta - \alpha)}{(1 - \alpha)(2 - \alpha)} \right], \quad (33)$$

$$\mathfrak{Z}_C^{1,-} = (b^2 - 1)^{-\Delta} [2\alpha + 2\Delta q_{2,1}(1)] = (b^2 - 1)^{-\Delta} 2\alpha \left[1 + \frac{\Delta(3 + \Delta - \alpha)}{(1 - \alpha)(2 - \alpha)} \right], \quad (34)$$

$$\mathfrak{Z}_C^+ = \frac{q_2(0)}{m_0 l_0} = -(2 - \alpha)(1 - \alpha)w_0, \quad (35)$$

$$\mathfrak{Z}_C^- = \frac{1}{(b^2 - 1)^2} \left[\frac{q_2(1)}{m_0 l_0} \right] = -\frac{(2 - \alpha)(1 - \alpha)\Sigma_0}{(b^2 - 1)^{2-\alpha}}. \quad (36)$$

It is essential to note that the value of the universal prefactor of the first-order confluent correction-to-scaling of Eq. 33 is only dependent of the values of the critical exponents α and Δ . Equations (33) to (36) lead to the following universal ratios:

$$\frac{A_1^+}{A_1^-} = \frac{\mathfrak{Z}_C^{1,+}}{\mathfrak{Z}_C^{1,-}} = (b^2 - 1)^\Delta, \quad (37)$$

$$\frac{A_0^+}{A_0^-} = \frac{\mathfrak{Z}_C^+}{\mathfrak{Z}_C^-} = (b^2 - 1)^{2-\alpha} \frac{w_0}{\Sigma_0}, \quad (38)$$

which explicit the specific roles of b^2 and $\frac{w_0}{\Sigma_0}$ in the parametric models of the scaled e.o.s..

In a similar manner, the two prefactors related to the Ising-like singular behaviors of the isothermal susceptibility above T_c are

$$\mathfrak{Z}_\chi^{1,+} = 2(\gamma - 1) + 2\Delta q_{1,1}(0) = 2(\gamma - 1), \quad (39)$$

$$\mathfrak{Z}_\chi^+ = \frac{q_1(0)}{m_0(l_0)^{-1}} = -2[(2 - \alpha)b^2w_0 + w_1]. \quad (40)$$

We note that this universal prefactor of the first-order confluent correction-to-scaling is only dependent of the value of the critical exponent γ . Equations (33) and (39) lead to the *intrinsic* universal ratio,

$$\frac{A_1^+}{\Gamma_1^+} = \frac{\mathfrak{Z}_C^{1,+}}{\mathfrak{Z}_\chi^{1,+}} = \frac{\alpha}{\gamma - 1} \left[1 + \frac{\Delta(3 + \Delta - \alpha)}{(1 - \alpha)(2 - \alpha)} \right], \quad (41)$$

only dependent of the critical exponent values. Therefore the corresponding ratio value (0.913263) is not conform to the MR value (0.941872) and specific to the so-called *intrinsic* CMM in the sense where the mathematical formulation of CMM implies that this amplitude ratio is only dependent of the critical exponents, a constraint not accounted for in the two main field-theoretical renormalization methods.

Now, in order to close our present construction of the CMM as close as possible to the MR mean crossover functions, it remains to reformulate the CPM universal quantities provided in Tables I to IV of Ref. [24] and to provide the needed additional universal quantities which extend the CMM estimates for the 26 amplitudes of Table 1.

2.3 Universal Parameter Sets for CMM Versus CPM

The universal values of the critical and mean-field exponents involved in the MR crossover functions are given in Table 2, which replaces Table I of Ref. [24]. For convenience, the CPM critical exponents are also reported in column 2 of present Table 2. We note that γ and ν are selected as the two independent exponents (to be conform with the universal features of the Ising-like critical limit).

The 20 amplitudes combinations and ratios considered in the present work are defined in column 2, lines 1 to 20 of Table 3. Lines 1 to 8 in part (a) give 8 universal ratios and combinations between 10 Ising-like leading amplitudes, while lines 9 to 14 in part (b) give 5 universal ratios between 7 first-order confluent amplitudes. In the latter case, 4 supplementary ratios are mentioned as combinations of the 5 previous ones. Lines 15 to 20 in part (c) give 6 universal ratios and combinations between 9 mean-field-like leading amplitudes (\overline{Q}_2 (line 20(e)) takes the same value above and below T_c). Also for convenience, the corresponding CPM values are reported in column 7 of Table 3 where the additional label (u) recalls for a universal quantity used in the construction of the CPM (with six universal parameters). The values used in the present CMM are given in column 3, while the MR values, or assumed MR-like values (and thus noted between brackets), calculated in the MR scheme are given in column 5. Line 10(i) indicates the irreducible (3%) failure of the parametric model in the estimate of the $\frac{A_1^+}{\Gamma_1^+}$ value only dependent of the critical exponents. Sign \equiv in Column 4, indicates 16 universal ratios and combinations exactly accounted for in the determination of the 16 universal parameters involved in the parametric

Table 3 20 universal amplitude combinations (column 2) for estimation of the CMM universal parameters given in Table (4)

1	2	3	4	5	6	7
		CMM	vs	MR		CPM
		This work		[17]	R%	[23, 24]
(a) Ising-like leading ratios or combinations						
1(e)	$\frac{A_0^+}{A_0^-} = U_0$	0.5368012	\equiv	0.5368012	0	0.52369(u)
2(e)	$\frac{\Gamma_0^+}{\Gamma_0^-} = U_2$	4.788337344	\equiv	4.788337344	0	4.94426(u)
3(e)	$\frac{\alpha A_0^+ \Gamma_0^+}{B_0^2} = R_C$	0.057406065	\equiv	0.057406065	0	0.0579693(u)
4(e)	$\Gamma_0^+ D_0^c B_0^{\delta-1} = R_\chi$ $\left(Q_1 = R_\chi^{-\frac{1}{\delta}}\right)$	1.7	\equiv	(1.7) (0.895446)	0	1.7066(u) (0.894753)
5(e)	$D_0^c (\Gamma_0^c)^\delta = (\delta)^{-\delta}$	5.30298 $\times 10^{-4}$	\equiv	5.30298 $\times 10^{-4}$	0	5.2826 $\times 10^{-4}$
6(e)	$\frac{\xi_0^+}{\xi_0^-} = U_\xi$	1.96	\equiv	(1.96)	0	(1.96)(u)
7(e)	$\alpha A_0^+ (\xi_0^+)^3 \frac{p_c}{k_B T_c} = Q^+$	0.01961673	\equiv	0.01961673	0	0.0188(u)
8(e)	$\left(\frac{\xi_0^c}{\xi_0^+}\right)^{2-\eta} \frac{\Gamma_0^+}{\Gamma_0^c} = Q_2$	1.17	\equiv	(1.17)	0	1.188
(b) Confluent correction ratios or combinations						
9(e)-(e1)	$\frac{A_1^+}{A_1^-} = (b^2 - 1)^\Delta$	1.20386	\equiv	1.20386	0	0.825171
10(i)	$\frac{A_1^+}{\Gamma_1^+} = \frac{\alpha}{\gamma-1} \left[1 + \frac{\Delta(3+\Delta-\alpha)}{(1-\alpha)(2-\alpha)}\right]$	0.913263	(\neq)	0.941872	-3	0.945429
11(e)	$\frac{\Gamma_1^+}{\Gamma_1^-}$	0.211618	\equiv	0.211618	0	0.154415
12(e)	$\frac{B_1}{\Gamma_1^+}$	0.9	\equiv	0.9	0	1.116155
13(?)	$\frac{\xi_1^+}{\Gamma_1^+}$	n.a	(?)	0.679191	< 0.3 (?)	
14(?)	$\frac{\xi_1^+}{\xi_1^-}$	n.a	(?)	(1)	< 0.3 (?)	
$\frac{10}{9}$ (i)	$\frac{A_1^-}{\Gamma_1^+}$	0.758861	(\neq)	0.782374	-3	1.145737
$\frac{10}{12}$ (i)	$\frac{A_1^+}{B_1}$	1.014737	(\neq)	1.04652	-3	0.84704
$\frac{10}{12}$ (i)	$\frac{A_1^-}{B_1}$	0.843179	(\neq)	0.869305	-3	
11 \times 12(e)	$\frac{B_1}{\Gamma_1^-}$	0.190456	\equiv	0.190456	0	
(c) mean-field-like leading ratios or combinations						
15(i)	$\frac{\overline{\Gamma_0^+}}{\overline{\Gamma_0^-}} = \overline{U_2}$	5.34037	(\neq)	2	167	2.056
16(e)	$\frac{\overline{\Delta C_V \Gamma_0^+}}{(\overline{B_0})^2} = \overline{R_C}$	$\frac{1}{2}$	\equiv	$\frac{1}{2}$	0	0.5109(u)

Table 3 (continued)

1	2	3	4	5	6	7
		CMM	vs	MR		CPM
		This work		[17]	R%	[23, 24]
17(e)	$\overline{\Gamma_0^+ D_0^c} (\overline{B_0})^2 = \overline{U^c} = \overline{R_x}$	1	\equiv	1	0	1.015
18(e)	$\overline{D_0^c} (\overline{\Gamma_0^c})^3 = \frac{1}{3^3}$	0.037037	\equiv	0.037037	0	
19(e)	$\frac{\overline{\xi_0^+}}{\overline{\xi_0^-}} = \overline{U_\xi}$	$\sqrt{2}$	\equiv	$\sqrt{2}$	0	$\sqrt{2}(u)$
20(e)	$\left(\frac{\overline{\xi_0^+}}{\overline{\xi_0^-}}\right)^2 \frac{\overline{\Gamma_0^+}}{\overline{\Gamma_0^c}} = \left(\frac{\overline{\xi_0^+}}{\overline{\xi_0^-}}\right)^2 \frac{\overline{\Gamma_0^-}}{\overline{\Gamma_0^c}} = \overline{Q_2}$	1	\equiv	(1)	0	1

Part (a) 8 Ising-like amplitude combinations; Part (b) 6 first-order confluent correction amplitude ratios (not available along the critical isotherm); Part (c) 6 mean-field-like amplitude combinations. Notations (e), (i) or (?) are for the exact induced or non available values of the amplitude combinations accounted in CMM (column 3), with reference to the corresponding RG estimates of Refs. [7, 17] (column 5). Column 4 compares columns 3 and 5 (see text) while residuals (expressed in %) are reported in column 6. Column 7: Recall of the related CPM values from Ref. [24] where the 10 CPM universal parameters control the 8 amplitude combination values (with additional label (u)), using the fixed values of $b^2 = 1.691047$ and $w_0 = -1$. In columns 5 and 7, () indicates a fixed value from a different source. This Table (column 3) must be used for CMM in place of Table II of Ref. [24] for CPM (recalled in column 7)

Eqs. 13 to 16. Signs (\neq), (\equiv) and (?) in Column 4, complemented by the values of the related residuals $R\%$ in column 6 indicate the induced results for the remaining 8 amplitudes ratios and combinations. Accordingly, additional (e), (i), and (n.a) indicate, respectively, the exact, induced or non-available account of each theoretical estimate provided by the MR scheme. Our Table 3 replaces and complements Table II of Ref. [24].

The CMM values of the 16 universal parameters involved in the parametric Eqs. 13 to 16 are reported in column 3 of Table 4. Lines 1 to 10 in part (a) of Table 4 give the values of 10 universal parameters involved in the CMM description of the thermodynamic properties. Lines 11 to 16 in part (b) give 6 universal parameters involved in the CMM crossover angular function of Eq. 16 for the correlation lengths. The unambiguous determination of these universal parameters is detailed in next Section and in Appendix A. As mentioned above, the closed procedure for their successive calculations account for 16 universal values characterizing the Ising-like critical limit (including the first-order confluent corrections to scaling) and the mean-field-like classical limit of the classical-to-critical crossover calculated in the MR scheme along the renormalized trajectory. The universal values of 5 auxiliary parameters introduced in the next section are also reported in lines 17 to 21 of part (c). Table 4 for the CMM case replaces and complements Table IV of Ref. [24] for the CPM case. As above, the CPM results are also recalled in column 4 of our present Table 4.

Finally, in column 2 of Table 5 are defined 26 universal prefactors involved in the determination of 26 physical amplitudes selected in Table 1 (using Agayan's

Table 4 Universal parameters involved in the parametric forms of intrinsic CMM

Parameters		CMM	CPM	Normed parameters	Line-step number
		this work	Table IV [24]	see Appendix A	see Table (8)
(a)	Thermodynamics				
1	b^2	(\otimes) 2.4472625381	1.691047	b^2	4
2	w_0	(\otimes) -0.327010546	-1	w_0^*	9
3	w_1	1.113948	1.504493	w_1^*	21
4	w_2	-0.55015526	-1.321901	w_2^*	52
5	w_3	-6.03256705	-0.1898336	w_3^*	51
6	w_4	7.36008178	0.05753347	w_4^*	50
7	w_5	-2.78995524	0	w_5^*	49
8	d	-1.2687866	0	d	43
9	e	4.11505	0	e	44
10	f	-2.55972	0	f	45
(b)	Correlations				
11	a_0	0.594073	0.064360	a_{r0}	25
12	a_1	0.289390	0.019119	a_{r1}	67
13	a_2	-0.148760	0	a_{r2}	68
14	a_0^*	0.487738	0.057984	a_{r0}^*	26
15	a_1^*	-0.562864	0.0016173	a_{r1}^*	69
16	a_2^*	1.37746	0	a_{r2}^*	70
(c)	Auxiliary				
17	Σ_0	-1.225658220	-0.94970813	$\Sigma_0^* = 1$	53
18	Σ_1	-5.187025250	-2.95735	Σ_1^*	16
19	Σ_2	-24.2823698	-15.327	Σ_2^*	46
20	S_0	-0.20186565	-4.94578	S_0^*	47
21	L_0	1.2865406	0	L_0^*	20

(a) 10 thermodynamic parameters used in Eqs. 13 to 15; (b) 6 correlation parameters used in Eq.(16); (c): 5 subparameters of Eqs. 23 to 27. This Table must be used for CMM on place of Table IV of Ref. [24] for CPM (here recalled in column 4). Column 5: notation of the corresponding normed parameter defined in Appendix A. Column 6: line-step number of Table 8 in Appendix A where is performed the unequivocal determination of the normed parameter

notations). Lines 1 to 10 of part (a) give 10 Ising-like leading prefactors, while lines 11 to 17 of part (b) give 7 first-order confluent prefactors. Lines 18 to 26 of part (c) give 9 mean-field-like leading prefactors. The universal values of the different prefactors are reported in column 3 for the present intrinsic CMM case and in column 5 for the ideal CMM (see below next section), while their identity (\equiv) or difference (\neq) are illustrated in column 4. The corresponding MR [17] and CPM [24] amplitude values are reported in columns 6 and 7, respectively. Table (5) for CMM case replaces and complements Table III of Ref. [24] for CPM case.

The 10 Ising-like leading amplitudes of part (a) are related by the 8 universal ratios and combinations of part (a) of Table 3. Two Ising-like amplitudes are then

Table 5 Universal values of 26 prefactors involved in the determination of the 26 amplitudes reported in Table 1

1	2	3	4	5	6	7
		intrinsic	vs	ideal	MR	CPM
		CMM	%	CMM	[17]	[24]
(a)	Ising-like prefactors					
1($e3+$)	$\frac{A_0^+}{m_0 l_0} = \mathfrak{Z}_C^+$	0.5511217	\equiv	$\mathbb{L}_m^d \Theta_m^{2-\alpha} Z_C^+$	$Z_C^+ = 1.719788$	1.68210
2($e3-$)	$\frac{A_0^-}{m_0 l_0} = \mathfrak{Z}_C^-$	1.02667754	\equiv	$\mathbb{L}_m^d \Theta_m^{2-\alpha} Z_C^-$	$Z_C^- = 3.203771$	3.21198
3($e4$)	$\frac{\Gamma_0^+}{m_0 (l_0)^{-1}} = \mathfrak{Z}_\chi^+$	0.7990253675	\equiv	$\mathbb{L}_m^d \Psi_m^2 \Theta_m^{-\gamma} (Z_\chi^+)^{-1}$	$(Z_\chi^+)^{-1} = 0.269571$	3.38317
4	$\frac{\Gamma_0^-}{m_0 (l_0)^{-1}} = \mathfrak{Z}_\chi^-$	0.16686906	\equiv	$\mathbb{L}_m^d \Psi_m^2 \Theta_m^{-\gamma} (Z_\chi^-)^{-1}$	$(Z_\chi^-)^{-1} = 0.0562974$	0.684260
5	$\frac{B_0}{m_0} = \mathfrak{Z}_M$	0.91372273	\equiv	$\mathbb{L}_m^d \Psi_m \Theta_m^\beta Z_M$	$Z_M = 0.937528$	3.28614
6	$\frac{D_0}{(m_0)^{-\delta} l_0} = \mathfrak{Z}_H$	2.99907597	\equiv	$\mathbb{L}_m^{-d\delta} \Psi_m^{-(\delta+1)} Z_H$	$[Z_H = 8.06073]$	0.00544595
7	$\frac{\Gamma_0^c}{m_0 (l_0)^{-\frac{1}{\delta}}} = \mathfrak{Z}_\chi^c$	0.16559269	\equiv	$\mathbb{L}_m^d \Psi_m^{\frac{\delta+1}{\delta}} Z_\chi^c$	$[Z_\chi^c = 0.134796]$	0.615451
8	$\frac{\xi_0^+}{(m_0 l_0)^{-\frac{1}{3}}} = \mathfrak{Z}_\xi^+$	0.68897	\equiv	$\mathbb{L}_m^{-1} \Theta_m^{-\nu} (Z_\xi^+)^{-1}$	$(Z_\xi^+)^{-1} = 0.471474$	0.466628
9	$\frac{\xi_0^-}{(m_0 l_0)^{-\frac{1}{3}}} = \mathfrak{Z}_\xi^-$	0.351515	\equiv	$\mathbb{L}_m^{-1} \Theta_m^{-\nu} Z_\xi^-$	$[Z_\xi^- = 0.240548]$	0.238076
10	$\frac{\xi_0^c}{(m_0 l_0)^{-\frac{1}{3}}} = \mathfrak{Z}_\xi^c$	0.335178	\equiv	$\mathbb{L}_m^{-1} \Psi_m^{\frac{1-\delta}{\delta(2-\eta)}} Z_\xi^c$	$[Z_\xi^c = 0.358975]$	0.214128
(b)	confluent prefactors					
11($e1+$)	$\frac{A_1^+}{g^{-\Delta_s}(1-\bar{u})} = \mathfrak{Z}_C^{1,+}$	0.437624	\neq -3.04	$\Theta_m^\Delta Z_C^{1,+}$ $\mathfrak{Z}_{m,C}^{1,+} = 0.451333$	$Z_C^{1,+} = 8.06569$	0.451915
12($e1-$)	$\frac{A_1^-}{g^{-\Delta_s}(1-\bar{u})} = \mathfrak{Z}_C^{1,-}$	0.3635164	\neq -3.04	$\Theta_m^\Delta Z_C^{1,-}$ $\mathfrak{Z}_{m,C}^{1,-} = 0.374904$	$Z_C^{1,-} = 6.69984$	0.547662
13($e2$)	$\frac{\Gamma_1^+}{g^{-\Delta_s}(1-\bar{u})} = \mathfrak{Z}_\chi^{1,+}$	0.479187	\equiv	$-\Theta_m^\Delta Z_\chi^{1,+}$	$Z_\chi^{1,+} = -8.56347$	0.478
14	$\frac{\Gamma_1^-}{g^{-\Delta_s}(1-\bar{u})} = \mathfrak{Z}_\chi^{1,-}$	2.2643938	\equiv	$-\Theta_m^\Delta Z_\chi^{1,-}$	$Z_\chi^{1,-} = -40.4666$	3.09555
15	$\frac{B_1}{g^{-\Delta_s}(1-\bar{u})} = \mathfrak{Z}_M^1$	0.43126813	\equiv	$\Theta_m^\Delta Z_M^1$	$Z_M^1 = 7.70712$	0.533522
16	$\frac{\xi_1^+}{g^{-\Delta_s}(1-\bar{u})} = \mathfrak{Z}_\xi^{1,+}$	n.a	\cong (< 0.3)	$-\Theta_m^\Delta Z_\xi^{1,+}$ $\mathfrak{Z}_{m,\xi}^{1,+} = 0.325459$	$Z_\xi^{1,+} = -5.81623$	
17	$\frac{\xi_1^-}{g^{-\Delta_s}(1-\bar{u})} = \mathfrak{Z}_\xi^{1,-}$	n.a	\cong (< 0.3)	$\Theta_m^\Delta Z_\xi^{1,-}$ $\mathfrak{Z}_{m,\xi}^{1,-} = 0.325459$	$[Z_\xi^{1,-} = 5.81623]$	
(c)	mean-field leading prefactors					
18	$\frac{\overline{\Delta C_V} g^{-\alpha}}{\bar{m}_0 l_0} = \overline{\mathfrak{Z}_{\Delta C_V}} = \overline{\mathfrak{Z}_C^-}$	0.516299	\neq 0.356	$\frac{\mathbb{L}_m^d \Theta_m^2 Z_{\Delta C, mf}^+}{\mathfrak{Z}_{m, \Delta C_V} = \overline{\mathfrak{Z}_{m,C}^-} = 0.514470}$	$Z_{\Delta C, mf}^- = 3$	1.97745
19	$\frac{\overline{\Gamma_0^+} g^{1-\gamma}}{\bar{m}_0 (l_0)^{-1}} = \overline{\mathfrak{Z}_\chi^+}$	0.973226	\neq 30.04	$\frac{\mathbb{L}_m^d \Psi_m^2 \Theta_m^{-1} (Z_{\chi, mf}^+)^{-1}}{\overline{\mathfrak{Z}_{m,\chi}^+} = 0.748403}$	$(Z_{\chi, mf}^+)^{-1} = 1$	3.75520

Table 5 (continued)

1	2	3	4	5	6	7
		intrinsic	vs	ideal	MR	CPM
		CMM	%	CMM	[17]	[24]
20	$\frac{\overline{\Gamma_0} g^{1-\gamma}}{\overline{m_0} l_0^{-1}} = \overline{\mathfrak{Z}_\chi^-}$	0.18224	\neq -51.3	$\frac{\mathbb{L}_m^d \Psi_m^2 \Theta_m^{-1} (Z_{\chi, mf}^-)^{-1}}{\overline{\mathfrak{Z}_{m, \chi}^-}} = 0.374202$	$(Z_{\chi, mf}^-)^{-1} = \frac{1}{2}$	1.82665
21	$\frac{\overline{B_0} g^{\beta-\frac{1}{2}}}{\overline{m_0}} = \overline{\mathfrak{Z}_M}$	1.00247	\neq 14.24	$\frac{\mathbb{L}_m^d \Psi_m \Theta_m^{\frac{1}{2}} Z_{M, mf}}{\overline{\mathfrak{Z}_{m, M}}} = 0.877531$	$Z_{M, mf} = \sqrt{6}$	3.81255
22	$\frac{\overline{D_0} g^{\frac{\delta-3}{2}}}{(\overline{m_0} l_0^{-3})} = \overline{\mathfrak{Z}_H}$	1.02245	\neq -0.631	$\frac{\mathbb{L}_m^{-3d} \Psi_m^{-4} Z_{H, mf}}{\overline{\mathfrak{Z}_{m, H}}} = 1.028939$	$[Z_{H, mf} = \frac{1}{6}]$	
23	$\frac{\overline{\Gamma_0^c} g^{-\alpha}}{\overline{m_0} l_0^{-\frac{1}{3}}} = \overline{\mathfrak{Z}_\chi^c}$	0.330876	\neq 0.211	$\frac{\mathbb{L}_m^d \Psi_m^{\frac{4}{3}} Z_{\chi, mf}^c}{\overline{\mathfrak{Z}_{m, \chi}^c}} = 0.330179$	$[Z_{\chi, mf}^c = \frac{2\frac{1}{3}}{3\frac{1}{3}}]$ (0.605707)	
24	$\frac{\overline{\xi_0^+} g^{\frac{1}{2}-\nu}}{(\overline{m_0} l_0)^{-\frac{1}{3}}} = \overline{\mathfrak{Z}_\xi^+}$	0.688970	\neq -0.286	$\frac{\mathbb{L}_m^{-1} \Theta_m^{-\frac{1}{2}} (Z_{\xi, mf}^+)^{-1}}{\overline{\mathfrak{Z}_{m, \xi}^+}} = 0.690946$	$(Z_{\xi, mf}^+)^{-1} = 1$	0.466628
25	$\frac{\overline{\xi_0^-} g^{\frac{1}{2}-\nu}}{(\overline{m_0} l_0)^{-\frac{1}{3}}} = \overline{\mathfrak{Z}_\xi^-}$	0.487175	\neq -0.286	$\frac{\mathbb{L}_m^{-1} \Theta_m^{-\frac{1}{2}} Z_{\xi, mf}^-}{\overline{\mathfrak{Z}_{m, \xi}^-}} = 0.488573$	$[Z_{\xi, mf}^- = \frac{\sqrt{2}}{2}]$	0.329956
26	$\frac{\overline{\xi_0^c} g^{\frac{1}{2}-\nu}}{(\overline{m_0} l_0)^{-\frac{1}{3}}} = \overline{\mathfrak{Z}_\xi^c}$	0.401722	\neq -12.22	$\frac{\mathbb{L}_m^{-1} \Psi_m^{-\frac{1}{3}} Z_{\xi, mf}^c}{\overline{\mathfrak{Z}_{m, \xi}^c}} = 0.457622$	$[Z_{\xi, mf}^c = \frac{2\frac{6}{1}}{3\frac{1}{3}}]$	0.272315

This Table (column 3) must be used for intrinsic CMM in place of Table III of Ref. [24] for CPM. In column 5 are given the analytical formulations to calculate the corresponding universal values of 26 prefactors for ideal CMM using only the three universal scale factors Θ_m , Ψ_m , and \mathbb{L}_m . In column 6, the universal amplitude values not involved through the limited number of calculated MR functions of Ref. [17], are noted between []. Column 1: ordering number (with added reference (*ei*, $i = \{1, 4\}$) for the four steps explicated in the text). $\overline{\mathfrak{Z}_C^+} = 0$ fixed

characteristics of the fluid system, as expected from the MR scheme. Similarly, among the 7 confluent amplitudes, only one is independent and characteristic of the confluent corrections-to-scaling (despite the fact that the numerical values of some universal ratios are not available). So that, only three amplitudes characterize the universality features of the simple fluid in the Ising-like limit. In the classical limit, introducing some additional constants (such as $\overline{\mathfrak{Z}_{B_{cr}}} = -2w_0$, $\overline{c_q^+} = 1$, and $\overline{A_0^+} = \overline{\mathfrak{Z}_C^+} = 0$, see Ref. [24] and CPM construction), among the 9 mean-field-like leading amplitudes only two mean-field amplitudes are fluid dependent according to a two parameters van der Waals-like e.o.s..

As detailed in Appendix A, we note that our closed analytical scheme provides the expected three parameter characterization of the CMM universality features in conformity with the three Ising-like parameter characterization of the MR scheme. Such

closed analytic scheme avoids the reference to the 3 fluid-dependent mean-field-like parameters m_0 , l_0 and $g = \frac{(\bar{u}\Lambda)^2}{c_t}$ (the latter one combining the physical crossover parameters \bar{u} and $\frac{\Lambda}{(c_t)^{\frac{1}{2}}}$) using now instead three master values $m_{m,0} = l_{m,0} = g_m = 1$, which agree with the infinite cutoff approximation $\Lambda \rightarrow \infty$, but $\bar{u} \rightarrow 0$, so that the product $\bar{u}\Lambda$ remains finite.

3 MR Crossover Forms of the Ideal CMM

3.1 Construction of Ideal CMM

The ideal matching between the respective Ising-like critical limits of the MR and the CMM crossover functions follows in a similar manner as in Ref. [18]. Indeed, the rescaling of their two theoretical scaling fields can be written

$$t = \Theta_m \Delta \tau^* \quad (42)$$

$$h = \Psi_m \Delta \tilde{\mu} \quad (43)$$

introducing thus the two scale factors Θ_m and Ψ_m , which characterize the so-called ideal CMM to be conform with the universal estimates of the Ising-like critical limit from the MR scheme. A universal quantity with subscript m refers to ideal CMM. Accordingly, the rescaling of their order parameter density field $\Delta \tilde{\rho} = \frac{\rho}{\rho_c} - 1$ is,

$$m = \Psi_m^{-1} \Delta \tilde{\rho} \quad (44)$$

The MR description of a simple fluid belonging to the one-component fluid subclass (labeled by the superscript $\{1f\}$ in Ref. [33]) assumes that the physical lengths are measured in unit of the (single) length scale $\alpha_c = \left(\frac{k_B T_c}{p_c}\right)^{\frac{1}{3}} = (v_0)^{\frac{1}{3}}$ and then related to the single MR wavelength scale g_0 through the following non-dimensional length $\mathbb{L}^{\{1f\}} = 25.585$ (see Eqs. 50, 93, and 94 of Ref. [33])

$$g_0 \alpha_c = \mathbb{L}^{\{1f\}} \quad (45)$$

Hence, the application of the ideal CMM can be extended to all the simple fluid subclass by assuming the identity

$$\mathbb{L}^{\{1f\}} \equiv \mathbb{L}_m \quad (46)$$

where \mathbb{L}_m is now the single dimensionless length scale introduced in the ideal CMM. Consequently, the three universal parameters Θ_m , Ψ_m , and \mathbb{L}_m characterize the MR universal forms (see below) of the ideal CMM applied to simple fluids. These forms are then calculated in quantitative conformity with the Ising-like two-scale-factor universality predicted by the MR scheme [7].

In order to suppress the non-universal character of the ideal CMM crossover functions, the preliminary step needs to introduce the following fixed values of physical parameters for CMM

$$m_{0,m} = 1 \quad (47)$$

$$l_{0,m} = 1 \quad (48)$$

$$g_m^{-\Delta} (1 - \bar{u}_m) = 1 \quad (49)$$

which induce the identities

$$f_{P,\text{Ising}}^l(m_{0,m}, l_{0,m}) \equiv 1 \quad (50)$$

$$f_{P,\text{CC}}^l(\Delta, g_m, \bar{u}_m) \equiv 1 \quad (51)$$

Using $\tilde{m}_0 = m_0 g^{\beta - \frac{1}{2}}$ and $\tilde{l}_0 = l_0 g^{\beta\delta - \frac{3}{2}}$ in the angular functions involved in the calculation of $\overline{P_0^l}$ leads to the rescaled quantities $\overline{f_{P,\text{mf}}^l(\tilde{m}_0, \tilde{l}_0)} \equiv \overline{f_{P,\text{mf}}^l(g, m_0, l_0)} = g^{x_{g,P}} \times \overline{f_{P,\text{Ising}}^l(m_0, l_0)}$, where $x_{g,P}$ is the corresponding exponent inferred by the $\{\tilde{m}_0, \tilde{l}_0\}$ combination in $\overline{f_{P,\text{mf}}^l(\tilde{m}_0, \tilde{l}_0)}$ (see for example Eq. 20 for the specific heat case). As expected from the CPM construction of the crossover function Y of Eq. 4, the classical asymptotic behavior of CMM is only normed by g , which acts as an effective Ginzburg number to define the validity range of the mean-field limit. Therefore, under the constraint $f_{P,\text{Ising}}^l(m_{0,m}, l_{0,m}) \equiv 1$, it is straightforward to obtain

$$\overline{f_{P,\text{mf}}^l(g_m, m_{0,m}, l_{0,m})} \equiv (g_m)^{x_{g,P}} \quad (52)$$

Therefore, a convenient choice

$$g_m \equiv 1 \quad (53)$$

$$\bar{u}_m \equiv 0 \quad (54)$$

corresponds to the infinite-cutoff approximation $\Lambda \rightarrow \infty$, with $\bar{u} \rightarrow 0$, so that the product $\bar{u}\Lambda$ remains finite. Indeed, in the infinite-cutoff approximation, the crossover behavior along the renormalized trajectory is controlled by a single crossover parameter associated to the lowest universal value of the confluent exponent Δ , that is precisely the case in the MR scheme.

The physical set $\{m_{0,m} = l_{0,m} = g_m = 1; \bar{u}_m = 0\}$ closes the construction of the MR universal forms of the ideal CMM crossover functions. For instance, along the critical isochore, the universal limiting forms of the ideal CMM crossover functions are thus written as follows

$$P_{m,Ising}^{\pm}(|\Delta\tau^*|) = P_{m,0}^{\pm}|\Delta\tau^*|^{-\pi_P} \left[1 + P_{m,1}^{\pm}|\Delta\tau^*|^{\Delta} \right] \quad (55)$$

$$\overline{P_{m,mf}^{\pm}(|\Delta\tau^*|)} = \overline{P_{m,0}^{\pm}|\Delta\tau^*|^{-\pi_{P,mf}}} \quad (56)$$

where the amplitudes $P_{m,0}^{\pm}$, $P_{m,1}^{\pm}$, and $\overline{P_{m,0}^{\pm}}$, are now universal quantities such as

$$P_{m,0}^{\pm} = \mathfrak{Z}_{m,X}^{\pm} \times 1 \quad (57)$$

$$P_{m,1}^{\pm} = \mathfrak{Z}_{m,X}^{1,\pm} \times 1 \quad (58)$$

$$\overline{P_{m,0}^{\pm}} = \overline{\mathfrak{Z}_{m,X}^{\pm}} \times 1 \quad (59)$$

According to the fact that the MR mean crossover functions are restricted to non-dimensional $P^l = \{c_V, \chi, m\}$ properties along the critical isochore, the next step needs to compare the universal crossover functions $P_m^{\pm}(\Delta\tau^*)$ for the ideal CMM case to the universal crossover functions $F_{P,MR}^{\pm}(t)$ for the MR case, using the equations

$$P_m^{\pm}(|\Delta\tau^*|) = Y_m^{\pm}(\mathbb{L}_m, \Theta_m, \Psi_m) F_{P,MR}^{\pm}(\Theta_m |\Delta\tau^*|) \quad (60)$$

In Eqs. 60, $Y_m^{\pm}(\mathbb{L}_m, \Theta_m, \Psi_m)$ are the normed combinations of the three universal parameters which result for the energy and length dimensions of the physical variables, while the two MR limiting behaviors of $F_{P,MR}^{\pm}(t)$ are given as follows

$$F_{P,MR,Ising}^{\pm}(|t|) = \mathbb{Z}_P^{\pm} |t|^{-\pi_P} \left[1 + \mathbb{Z}_P^{1,\pm} |t|^{\Delta} \right] \quad (61)$$

$$F_{P,MR,mf}^l(|t|) = \mathbb{Z}_{P,mf}^{\pm} |t|^{-\pi_{P,mf}} \quad (62)$$

The term to term comparisons of Eqs. 55 and 56 with Eqs. 61 and 62 using additional conditions of Eqs. 57, 58, and 59, induce the following results

$$\mathfrak{Z}_{m,P}^{\pm} = \mathbb{Z}_P^{\pm} \times Y_{m,Ising}^{\pm}(\mathbb{L}_m, \Theta_m, \Psi_m) (\Theta_m)^{-\pi_P} \quad (63)$$

$$\mathfrak{Z}_{m,P}^{1,\pm} = \mathbb{Z}_P^{1,\pm} \times (\Theta_m)^{\Delta} \quad (64)$$

$$\overline{\mathfrak{Z}_{m,P}^{\pm}} = \overline{\mathbb{Z}_{P,mf}^{\pm}} \times Y_{m,mf}^{\pm}(\mathbb{L}_m, \Theta_m, \Psi_m) (\Theta_m)^{-\pi_{P,mf}} \quad (65)$$

The corresponding results now extended to the complete set of 26 amplitudes selected in Table 1 are reported in column 5 of Table 5.

A refined analysis of the Ising-like limit shows that the readily independent leading prefactors are $\mathfrak{Z}_{m,C}^+$ and $\mathfrak{Z}_{m,\chi}^+$ (as α and γ are the corresponding independent exponents), while the MR universal form of ideal CMM uses $\mathfrak{Z}_{m,\chi}^{1,+}$ as the entry data to start the MR versus CMM exact matching. Indeed, the MR universal form of

ideal CMM is defined in a unequivocal manner by considering the restricted two-term master forms of the Ising-like singular behaviors of the specific heat above and below T_c and the isothermal susceptibility above T_c , i.e.,

$$c_{V,m}^{\pm}(\Delta\tau^*) = \mathfrak{Z}_{m,C}^{\pm}(\Delta\tau^*)^{-\alpha} \left[1 + \mathfrak{Z}_{m,C}^{1,\pm}(\Delta\tau^*)^{\Delta} \right] \quad (66)$$

$$\chi_{T,m}^+(\Delta\tau^*) = \mathfrak{Z}_{m,\chi}^+(\Delta\tau^*)^{-\gamma} \left[1 + \mathfrak{Z}_{m,\chi}^{1,+}(\Delta\tau^*)^{\Delta} \right] \quad (67)$$

As demonstrated in Appendix A, we can then successively calculate in four steps (labelled (ei), with $i = \{1, 4\}$) the four following quantities knowing the MR Ising-like critical limit:

(e1) MR universal ratio $\frac{A_1^+}{A_1^-} = 1.20386$ fixes the value $b^2 = 2.4472625381$ for intrinsic CMM, when $\frac{A_1^+}{A_1^-}$ was used as entry data in the equation

$$\frac{A_1^+}{A_1^-} = \frac{\mathfrak{Z}_{m,C}^{1,+}}{\mathfrak{Z}_{m,C}^{1,-}} \equiv \frac{\mathfrak{Z}_C^{1,+}}{\mathfrak{Z}_C^{1,-}} = (b^2 - 1)^{\Delta} \quad (68)$$

where $\mathfrak{Z}_C^{1,+}$ and $\mathfrak{Z}_C^{1,-}$ are explicited from CMM angular functions (see lines 11(e1+) and 12(e1-) in Table 6);

(e2) MR confluent amplitude $\mathbb{Z}_{\chi}^{1,+} = 8.56347$ fixes the value $\Theta_m = 0.003199934$ for ideal CMM, when $\mathfrak{Z}_{\chi}^{1,+} = 2(\gamma - 1)$ was used as entry data (see line 13(e2) in Table 6) in the equation

$$\mathbb{Z}_{\chi}^{1,+}(\Theta_m)^{\Delta} \equiv \mathfrak{Z}_{\chi}^{1,+} = 2(\gamma - 1) = 0.479187 \quad (69)$$

However, this (e2) step also reveal one irreducible difference between ideal and intrinsic CMM noted previously

(e3) MR leading amplitude $\mathbb{Z}_C^+ = 1.719788$ fixes the value $w_0 = -0.327011$ for intrinsic CMM, when \mathbb{Z}_C^+ was used as entry data (see line 1n(e3n(+)) in Table (6)) in the term to term matching equation

$$\mathfrak{Z}_{m,C}^+ = \alpha \mathbb{Z}_C^+(\mathbb{L}_m)^d (\Theta_m)^{2-\alpha} \equiv \mathfrak{Z}_C^+ = -(2 - \alpha)(1 - \alpha)w_0 = 0.551122 \quad (70)$$

using previous values of $\mathbb{L}_m = 25.585$ and $\Theta_m = 0.003199934$ for ideal CMM. Similarly, the MR-leading amplitude $\mathbb{Z}_C^- = 3.203771$ fixes the value $\Sigma_0 = \frac{\tilde{w}(1)}{\tilde{m}_0 \tilde{l}_0} = -1.22565822$ for intrinsic CMM, when \mathbb{Z}_C^- was used as entry data (see line 2n(e3(-)) in Table 6) in the term to term matching equation

$$\mathfrak{Z}_{m,C}^- = \alpha \mathbb{Z}_C^-(\mathbb{L}_m)^d (\Theta_m)^{2-\alpha} \equiv \mathfrak{Z}_C^- = -\frac{(2 - \alpha)(1 - \alpha)}{(b^2 - 1)^{2-\alpha}} \Sigma_0 = 1.02667754 \quad (71)$$

More generally, as demonstrated in Appendix, the thermodynamic description using intrinsic CMM above and below T_c is closed at this iii) level, as the two independent

universal parameters (b^2 and w_0 or Σ_0) are known. Then, all the 8 remaining universal parameters can be calculated, with especial attention to $w_1 = 1.113948$ which result from the unique solution of the auxiliary quantity $\frac{L_0}{\Sigma_0}$ considering the Ising like and the mean-field like estimations of $\frac{\tilde{w}^*(0)}{\tilde{m}_0 \tilde{l}_0} = w_1$ (see also Appendix). Finally,

(e4) MR-leading amplitude $\left(\mathbb{Z}_\chi^+\right)^{-1} = 3.709601$ fixes the value $\Psi_m = 3.781467 \times 10^{-4}$ for ideal CMM, when it was used as entry data (see line 3n(e4) in Table 6) in the term to term matching equation

$$\mathfrak{Z}_{m,\chi}^+ = \left(\mathbb{Z}_\chi^+\right)^{-1} (\mathbb{L}_m)^d (\Psi_m)^2 (\Theta_m)^{-\gamma} \equiv \mathfrak{Z}_\chi^+ = -2[(2-\alpha)b^2w_0 + w_1] = 0.799025 \quad (72)$$

After the (e4) step, the following set of universal values

$$\begin{aligned} \mathbb{L}_m &= 25.585 \\ \Theta_m &= 0.003199934 \\ \Psi_m &= 3.781467 \times 10^{-4} \end{aligned} \quad (73)$$

closes the MR universal description of the Ising-like critical limit of the ideal CMM whatever the line l , as expected in Ref. [34].

3.2 Intrinsic CMM Versus Ideal CMM

The results of the comparison between the 26 prefactor values of the intrinsic CMM and ideal CMM for the 26 selected amplitudes were reported in column 3 and 5 of Table 5. The following table forms

Intrinsic CMM	?	Ideal CMM
\mathfrak{Z}_P^l	10 Yes	$\mathfrak{Z}_{m,P}^l$
$\mathfrak{Z}_P^{1,l}$	2 No & 5 Yes	$\mathfrak{Z}_{m,P}^{1,l}$
$\overline{\mathfrak{Z}_P^l}$	9 No	$\overline{\mathfrak{Z}_{m,P}^l}$

summarizes the comparison where 10 Ising-like prefactors are identical, only 5 among the 7 confluent prefactors are identical, and 9 mean-field-like prefactors are different.

3.2.1 Ising-Like Singular Limit

As expected, the Ising-like leading limit is perfectly accounted for both intrinsic and ideal CMM. Two (\mathfrak{Z}_C^+ and \mathfrak{Z}_χ^+) among the ten \mathfrak{Z}_P^l prefactors are independent since the other 8 prefactor ratios and combinations of Part (a) in Table 5 are in agreement with the two-scale-factor universality (accounted for by our choice of

α and γ as independent exponents). $\mathfrak{Z}_P^l \equiv \mathfrak{Z}_{m,P}^l$ for any P^l and subscript m can be suppressed for these Ising-like leading prefactors. The numerical values of these ten \mathfrak{Z}_P^l prefactors are thus obtained from the universal values of the two MR-independent amplitudes $\left(\mathbb{Z}_\chi^+\right)^{-1} = 0.269571$, $\mathbb{Z}_C^+ = 1.719788$ [17, 33] (see Appendix A)

We note that the CMM Ising-like leading amplitude $\frac{A_0^+}{m_0 l_0} = \mathfrak{Z}_C^+ = -(2 - \alpha)(1 - \alpha)w_0 = \mathfrak{Z}_C^{*,+} \times \Sigma_0 = 0.551122$ of the specific heat in the homogeneous domain is only characterized by Σ_0 (or w_0 , equivalently, using Eqs. 70 and/or 71). Therefore, Σ_0 or w_0 take scale factor nature similar to A_0^+ involved in the hyperscaling law $\alpha \mathfrak{Z}_C^+(\xi_0^+)^3 = Q^+$. This result is to conform with our choice of $\alpha_c = \left(\frac{k_B T_c}{p_c}\right)^{\frac{1}{3}}$ as a single length unit of each selected simple fluid, introducing then the single master value \mathbb{L}_m (see Eq. 46) for the simple fluid universality subclass.

3.2.2 Ising-Like Confluent Corrections

The origin of the +3% difference for the two confluent amplitudes $\mathfrak{Z}_C^{1,\pm}$ from reference to $\mathfrak{Z}_{m,C}^{1,\pm}$ (see lines 11 and 12 in Table 5) is due to the irremediable default previously mentioned in intrinsic CMM where the calculated value of the universal ratio $\frac{A_0^+}{\Gamma_1^+}$ only depends on the critical exponent values (see Eq. 41). However, the intrinsic entry prefactor $\mathfrak{Z}_\chi^{1,+} = 2(\gamma - 1)$ well remains the single independent prefactor to characterize the first-order confluent corrections to scaling, as the ideal entry prefactor $\mathfrak{Z}_{m,\chi}^{1,+}$ is thus obtained only from the universal value of the MR independent amplitude $\mathbb{Z}_\chi^{1,+} = 8.56347$.

For the critical limit $\Delta T^* \rightarrow 0$, the ideal matching of the correlation functions needs to perform the term to term comparison of the two following equations

$$\mathfrak{Z}_{m,\xi}^+ = \left(\mathbb{Z}_\xi^+\right)^{-1} (\mathbb{L}_m)^{-1} (\Theta_m)^{-\nu} = 0.68897 \equiv \mathfrak{Z}_\xi^+ = \sqrt{a_{r0}(-2[2bw_0 + w_1])} = 0.68897 \quad (74)$$

$$\mathfrak{Z}_{m,\xi}^{1,+} = - \left(\mathbb{Z}_\xi^{1,+}\right)^{-1} (\Theta_m)^\Delta = 0.325459 \stackrel{?}{=} \mathfrak{Z}_{m,\xi}^{1,+} = \text{non available} \quad (75)$$

If $\mathfrak{Z}_{m,\xi}^+ \equiv \mathfrak{Z}_\xi^+$ (see Eq. 74) as expected just above for the leading amplitude, the CMM value of the confluent amplitude $\mathfrak{Z}_{m,\xi}^{1,+}$ is difficult to obtain analytically, due to the complex functional forms of the crossover Eq. 12. The case of $\mathfrak{Z}_{m,\xi}^{1,-}$ is similar.

Therefore, the control of the universal MR ratio $\frac{\xi_1^+}{\Gamma_1^+} = \frac{\mathbb{Z}_\xi^{1,+}}{\mathbb{Z}_\xi^{1,+}} = 0.679191$ [17, 33] and the fixed ratio $\frac{\xi_1^+}{\xi_1^-} = \frac{\mathbb{Z}_\xi^{1,+}}{\mathbb{Z}_\xi^{1,-}} = 1$ in Column 5 of Table 3 are not checked here (see lines labeled 13(?) and 14(?) in column 3 of Table 3).

We note that the perfect matching of the 2-term Ising-like singular behavior of the isothermal susceptibility above and below T_c in the intrinsic CMM case is one of the noticeable confluent ameliorations from the CPM case.

3.2.3 Mean-Field-Like Classical Limit

The actual mean-field behavior resulting from the calculated crossover MR functions of Ref. [17] leads to the amplitude values $\overline{Z}_\chi^+ = 1$, $\overline{Z}_\chi^- = 2$, $\overline{Z}_M^+ = \sqrt{6}$, with the specific heat jump $\overline{Z}_{\Delta C_V} = \overline{Z}_{C, mf}^- - \overline{Z}_{C, mf}^+ = 6,79349 - 3,79004 = 3,00345$ slightly different from $\overline{Z}_C^- = \overline{Z}_{C, mf}^- - X_{C^-} = 6,79349 - 3,793494 = 3$, which corresponds to the correct jump with the fixed value $\overline{Z}_C^+ = \overline{A}_0^+ = 0$ (see column 6 of Table 5). This specific jump difference results from the MR background constant difference $X_{C^+} = -3,79829 \neq X_{C^-} = -3,79349$ involved in the calculated crossover functions C^* of the specific heat in the homogeneous and non-homogeneous domains (see Tables I and II of Ref. [17]). The supplementary values between [] can be estimated using appropriate amplitude combinations of part (c) of Table 3.

The resulting mean-field prefactors of ideal CMM are given in column 5 of Table 5, while the ones of intrinsic CMM are given in column 3 of same Table 5. All these mean-field prefactors are different since $\overline{Z}_P^l \neq \overline{Z}_{m, P}^l$ for any P^l (see text and table forms just above), with related (small or large) residuals $r\% = 100 \times \left[\frac{\overline{Z}_P^l}{\overline{Z}_{m, P}^l} - 1 \right]$ reported in column 4 of Table 5. Especially considering the susceptibility case along the critical isochore, the residuals reach 30% and 50% above and below T_c , mainly due to the fact that the $\overline{U}_2 = \frac{\Gamma_0^+}{\Gamma_0^-}$ value cannot be accounted for in the construction of intrinsic CMM (see Appendix A). Despite the large uncorrected value (167% discrepancy) of this \overline{U}_2 ratio, all the remaining 5 classical amplitude combinations and ratios of Table 3 remain accounted for exactly in this construction. An essential result for a better understanding of the number of fluid dependent parameters is introduced in the parametric crossover model to characterize the classical limit.

Similarly, the prefactor $\overline{Z}_{B_{cr}}^* = \frac{\overline{Z}_{B_{cr}}}{\Sigma_0}$ (see Eq. 17) related to the analytic background constant of intrinsic CMM differs from the resulting prefactor of ideal CMM calculated as follows:

$$\overline{Z}_{m, B_{cr}} \equiv \overline{Z}_{m, \Delta C_V} = \overline{Z}_{m, C}^- = \overline{Z}_{\Delta C_V}^+ (\mathbb{L}_m)^d (\Theta_m)^2 \quad (76)$$

with the use of the scale factors of Eq. 73. Here, the residuals is small (0.356 %), as the MR mean-field amplitude $\overline{Z}_{C, mf}^+ = 3,79829$ of the MR function C^* of the specific heat in the homogeneous domain is quasi-corrected by the background constant $X_C = -3,79004$ to generate a mean-field limit $\overline{Z}_C^+ = \overline{Z}_{C, mf}^+ + X_{C^+} = 0,00825$

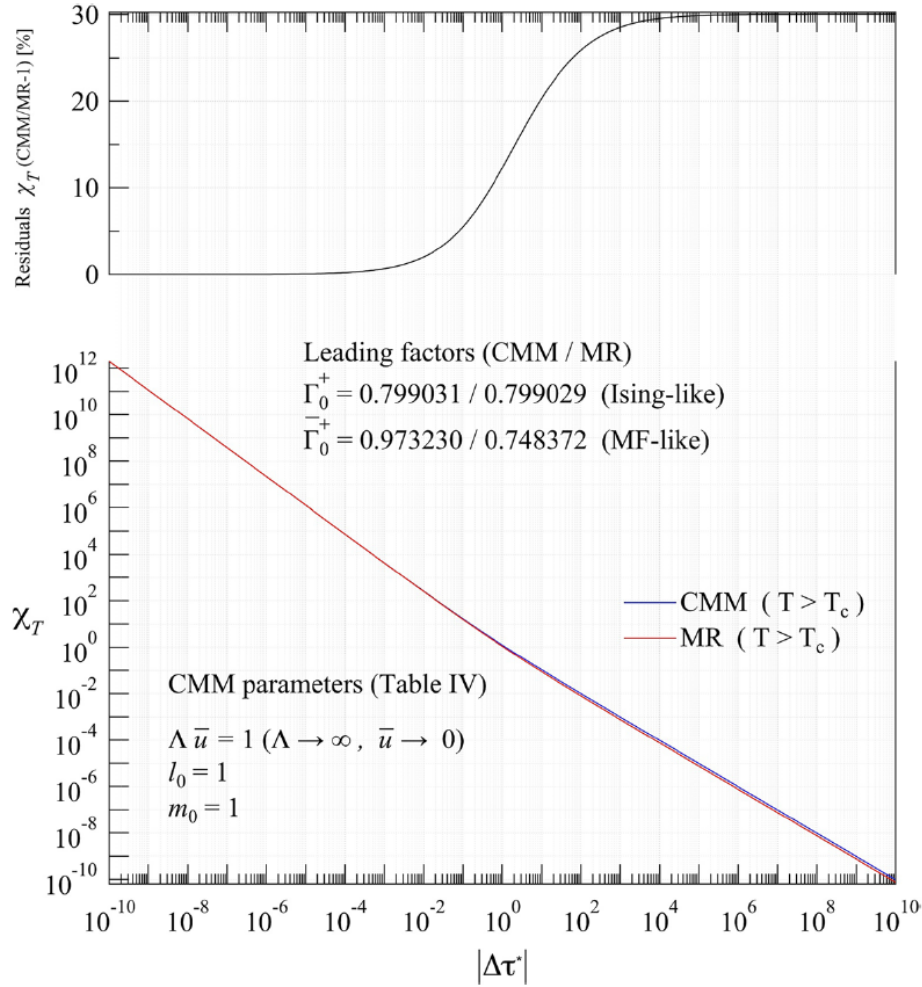


Fig. 1 Comparison of the isothermal susceptibility χ^* in the homogeneous domain calculated from intrinsic CMM (blue curve labelled CMM) and ideal CMM (red curve labelled MR), the latter being obtained (see text) from the corresponding MR crossover function χ^* (see Table I of Ref. [17]). The residuals, $\chi_T^{*\%} = 100 \times \left[\frac{\chi_T^{*(CMM)}}{\chi_T^{*(MR)}} - 1 \right]$ are shown in the top part plot

not exactly conform with the CMM fixed value $\overline{A}_0^+ = 0$. Accordingly, $\overline{\mathfrak{Z}}_C^+ = -0.00141479 \neq 0$.

3.2.4 Complete Crossover Behavior

The comparison between the results obtained from intrinsic CMM and ideal CMM is made through the Figs. 1 to 15.

For ideal CMM case, the results (see red curves) are obtained from the scale dilatation of the MR mean crossover functions defined in Table I and II of Ref. [17], using then the master scale factors \mathbb{L}_m , Θ_m , and Ψ_m (see Eq. 73).

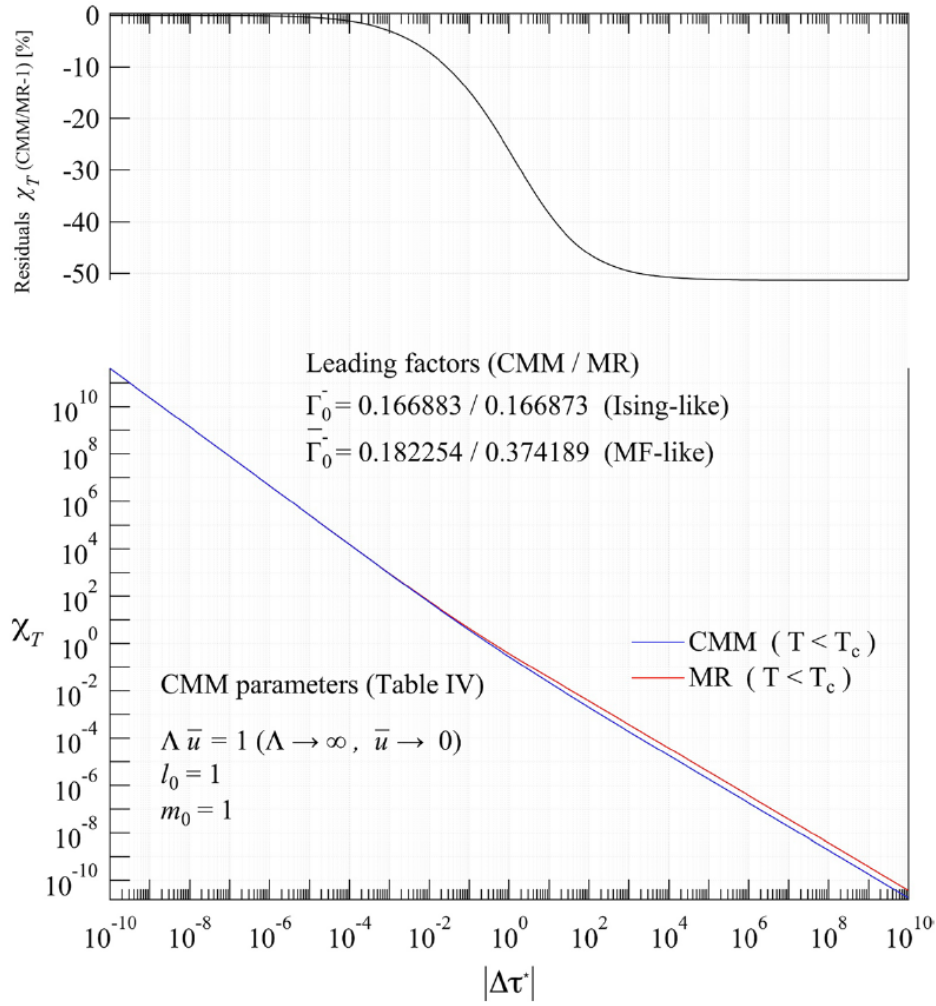


Fig. 2 Same as Fig. 1 for the isothermal susceptibility χ^* in the non homogeneous domain (tired curves) calculated from intrinsic CMM (black curve) and ideal CMM (red curve), the latter being obtained (see text) from the corresponding MR crossover function χ^* (see Table I of Ref. [17]). The residuals, $\chi_T^* \% = 100 \times \left[\frac{\chi_T^{*(CMM)}}{\chi_T^{*(MR)}} - 1 \right]$ are shown in the top part plot

The related residuals rP^t of each crossover function P^t is illustrated on the top part of each figure. We note that $r\pi_{e,P} \% = 100 \times \left[\frac{\pi_{e,P,CMM}}{\pi_{e,P,MR}} - 1 \right]$ for all the properties except for the specific heat where the absolute difference $\delta C_V = 1000 \times [C_{V,CMM} - C_{V,MR}]$ seems more appropriate for such a low divergence with significant background contribution. In the first four Figs. 1 to 4 are reported the corresponding crossover functions $\chi^{*,+}$ and $C^{*,+}$ in the homogeneous domain and $\chi^{*,-}$ and $C^{*,-}$ in the non-homogeneous domain, respectively.

In the Fig. 1, the inverse susceptibility in the homogeneous domain reads

$$[\chi_{idealCMM}^+(\Delta\tau^*)]^{-1} \equiv (\chi_{MR}^+)^{-1} = (\mathbb{L}_m)^{-d} (\Psi_m)^{-2} [\chi^*(\Theta_m \Delta\tau^*)]^{-1} \quad (77)$$

where $1/\chi^*(t)$ is defined from Eqs. (5) and (6) of Ref. [17], with the related parameters of column 4 in Table I (accounting for the modifications noted on Ref. [40]) and $t = \Theta_m \Delta\tau^*$. From Eq. 78, the pure leading singular behavior for $\Delta\tau^* \rightarrow 0$ reads

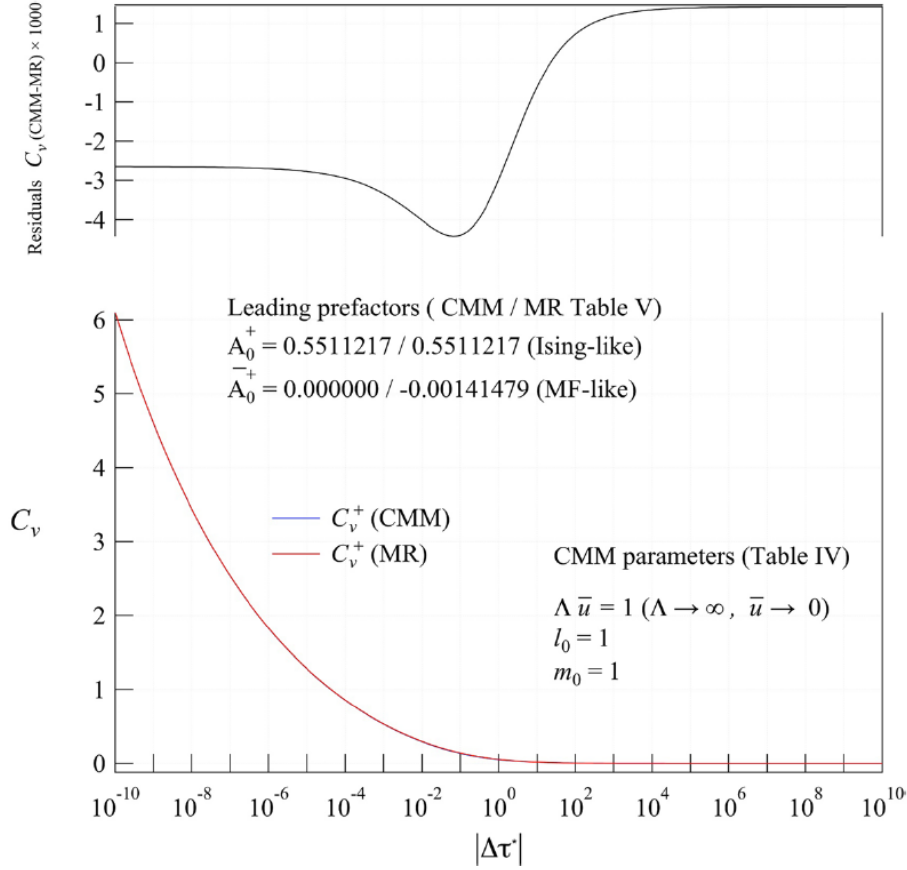


Fig. 3 Same as Fig 1 for the heat capacity case C^+ in the homogeneous domain, except the absolute difference $\delta C^* = 1000 \times [C^{*,+}(\text{CMM}) - C^{*,+}(\text{MR})]$ shown in the top part plot

$$(\chi_{\text{idealCMM}}^+)_{\Delta\tau^* \rightarrow 0}^{-1} = (\mathbb{L}_m)^{-d} (\Psi_m)^{-2} (\mathbb{Z}_\chi^+) (\Theta_m)^\gamma (\Delta\tau^*)^\gamma = (\mathfrak{Z}_\chi^+)^{-1} (\Delta\tau^*)^\gamma \quad (78)$$

while the pure leading classical behavior for $\Delta\tau^* \rightarrow \infty$ reads

$$(\chi_{\text{idealCMM}}^+)_{\Delta\tau^* \rightarrow \infty}^{-1} = (\mathbb{L}_m)^{-d} (\Psi_m)^{-2} (\mathbb{Z}_{\chi,\text{mf}}^+) \Theta_m \Delta\tau^* = (\overline{\mathfrak{Z}_{m,\chi}^+})^{-1} \Delta\tau^* \quad (79)$$

The equivalent Fig. 3 for specific heat in the homogeneous domain needs a particular attention to the role of the additive constant X_{C^+} . Indeed the above equivalent results for C^+ read

$$\left\{ \begin{array}{l} [C_{\text{idealCMM}}^+(\Delta\tau^*)] \equiv C_{\text{MR}}^{*,+} = (\mathbb{L}_m)^d (\Theta_m)^2 C^{*,+} (\Theta_m \Delta\tau^*) \\ C_{\text{idealCMM},\Delta\tau^* \rightarrow 0}^+ \equiv C_{\text{MR},\Delta\tau^* \rightarrow 0}^{*,+} = (\mathbb{L}_m)^d (\mathbb{Z}_C^+) (\Theta_m)^2 (\Theta_m)^{-\alpha} |\Delta\tau^*|^{-\alpha} + (\mathbb{L}_m)^d (\Theta_m)^2 X_{C^+} \\ \quad = \mathfrak{Z}_C^+ |\Delta\tau^*|^{-\alpha} - 0.651368 \\ C_{\text{idealCMM},\Delta\tau^* \rightarrow \infty}^+ \equiv C_{\text{MR},\Delta\tau^* \rightarrow \infty}^{*,+} = (\mathbb{L}_m)^d (\Theta_m)^2 (\mathbb{Z}_{C,\text{mf}}^+ + X_{C^+}) \equiv \overline{\mathfrak{Z}_C^+} \lesssim 0 \end{array} \right. \quad (80)$$

where the significant contribution of the background constant $(\mathbb{L}_m)^d (\Theta_m)^2 X_{C^+} = -0.651368$ is explicated in the second equation.

In the last equation, the CMM constraint $A_0^+ = 0$ is not exactly satisfied since $C_{\text{idealCMM}, \Delta\tau^* \rightarrow \infty}^+ \equiv \overline{\mathfrak{Z}}_C^+ = -0.00141479 \neq 0$, due to the quoted non-zero value of $Z_{C,\text{mf}}^+ + X_{C^+} = -0.00824$ (see above). These effects are illustrated on this figure by the small non-zero value of $\delta C_V = 1000 \times [C_{V,\text{CMM}} - C_{V,\text{MR}}]$ at both limits.

The formulation of the corresponding equations for the non-homogeneous domain is similar, noting that the background term for the specific heat for ideal CMM takes the value $(\mathbb{L}_m)^d (\Theta_m)^2 X_{C^-} = -0.650545$, leading to the related mean-field-like limit

$$\begin{aligned} C_{\text{idealCMM}, \Delta\tau^* \rightarrow \infty}^- &= C_{\text{MR}, \Delta\tau^* \rightarrow \infty}^{*,-} \\ &= (\mathbb{L}_m)^d (\Theta_m)^2 (Z_{C,\text{mf}}^- + X_{C^-}) \equiv \overline{\mathfrak{Z}}_C^- = 1.165014 - 0.650545 \\ &= 0.414469 \end{aligned} \quad (81)$$

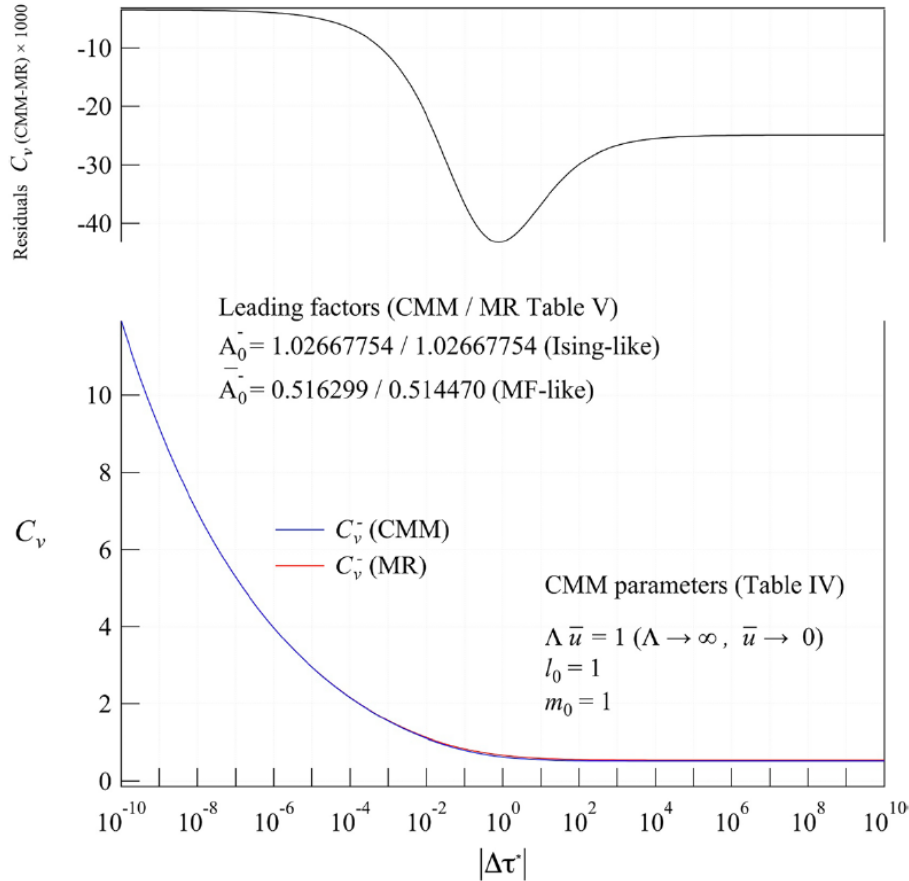


Fig. 4 Same as Fig 2 for the heat capacity case C^- in the non homogeneous domain, except the absolute difference $\delta C^* = 1000 \times [C^{*,-}(\text{CMM}) - C^{*,-}(\text{MR})]$ shown in the top part plot

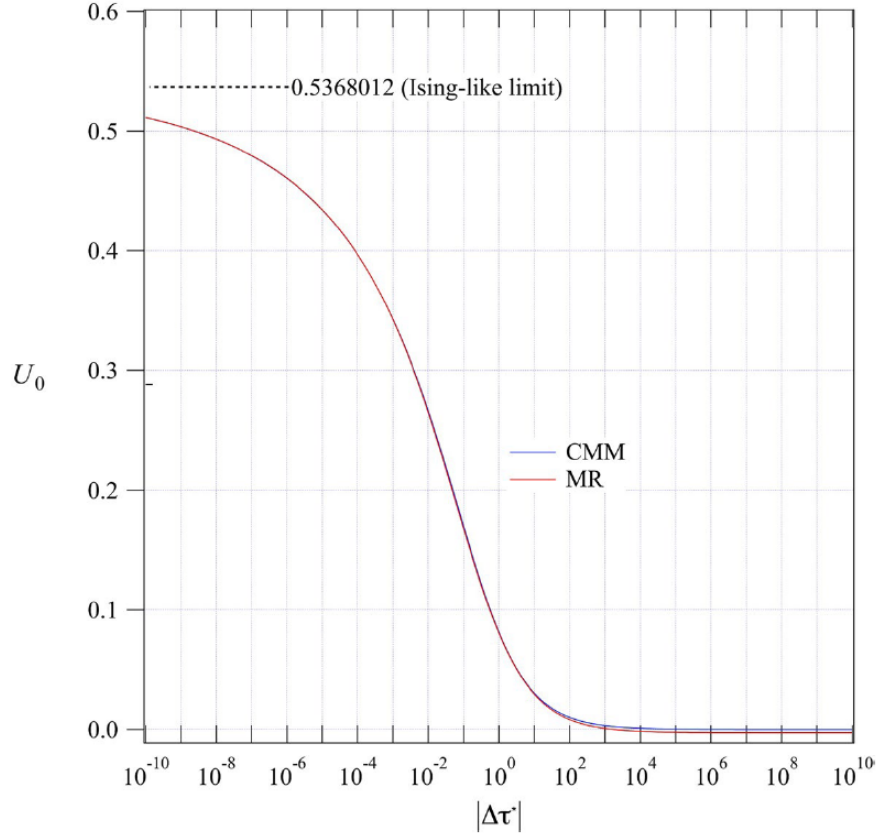


Fig. 5 Universal amplitude ratio U_0 calculated from intrinsic CMM (blue curve labelled CMM) and ideal CMM (red curve labelled MR), the latter being obtained (see text) from the corresponding MR crossover functions

As a result, in Figs. 5 and 6 are illustrated their corresponding universal ratios $U_0 = \frac{C^{*,+}}{C^{*, -}}$ and $U_2 = \frac{\chi^{*,+}}{\chi^{*, -}}$.

The Ising limit $U_0 = 0.5368012$ (see Table 3) is not reached at $\Delta\tau^* = 10^{-10}$ (where $U_{0,e} = 0.511408$), certainly due to the large confluent+background effects observed on each specific heat property calculated from the MR crossover functions above and below T_c .

The situation is distinct for the U_2 ratio due to the uncontrolled intrinsic mean-field limit $\underline{U}_{2,CMM} = 5.34037$, which differs significantly from the MR calculated value $\underline{U}_{2,MR} = 2$.

The analysis of the crossover effects of such uncontrolled mean-field limits will be made in a future work.

In the two Figs. 7 and 8 are reported the corresponding crossover functions $\xi^{*,+}$ in the homogeneous domain and $m^*(MR67)$ in the non-homogeneous domain, with their associated residuals, respectively.

For the m^* case, the equivalent equations to Eqs. 80 for the order parameter density (coexistence curve) read

$$\left\{ \begin{aligned} [(\Delta\tilde{\rho}_{LV})_{\text{idealCMM}}(\Delta\tau^*)] &= \frac{\rho_L - \rho_V}{2\rho_c} \equiv m_{\text{MR}}^* \\ &= (\underline{\mathbb{L}}_m)^d (\Psi_m)^2 m_{\text{MR67}}^* (\Theta_m |\Delta\tau^*|) \\ (\Delta\tilde{\rho}_{LV})_{\text{idealCMM}, \Delta\tau^* \rightarrow 0} &= m_{\text{MR}, \Delta\tau^* \rightarrow 0}^* \\ &= (\underline{\mathbb{L}}_m)^d (\Psi_m)^2 (\mathbb{Z}_M) (\Theta_m)^\beta |\Delta\tau^*|^\beta \\ &= \mathbb{Z}_M^- |\Delta\tau^*|^\beta \\ (\Delta\tilde{\rho}_{LV})_{\text{idealCMM}, \Delta\tau^* \rightarrow \infty} &= m_{\text{MR}, \Delta\tau^* \rightarrow \infty}^* \\ &= (\underline{\mathbb{L}}_m)^d (\Psi_m)^2 (\mathbb{Z}_{M, \text{mf}}) (\Theta_m)^{\frac{1}{2}} |\Delta\tau^*|^{\frac{1}{2}} \\ &= \mathbb{Z}_{m, M}^+ |\Delta\tau^*|^{\frac{1}{2}} \end{aligned} \right. \quad (82)$$

where $m_{\text{MR67}}^*(t)$ is defined from Eqs. (5) and (6) of Ref. [17], with the related parameters of column 4 in Table II (accounting for the modifications noted on Ref. [40]) and $t = \Theta_m |\Delta\tau^*|$. The thermodynamic derivation of the symetrized order parameter

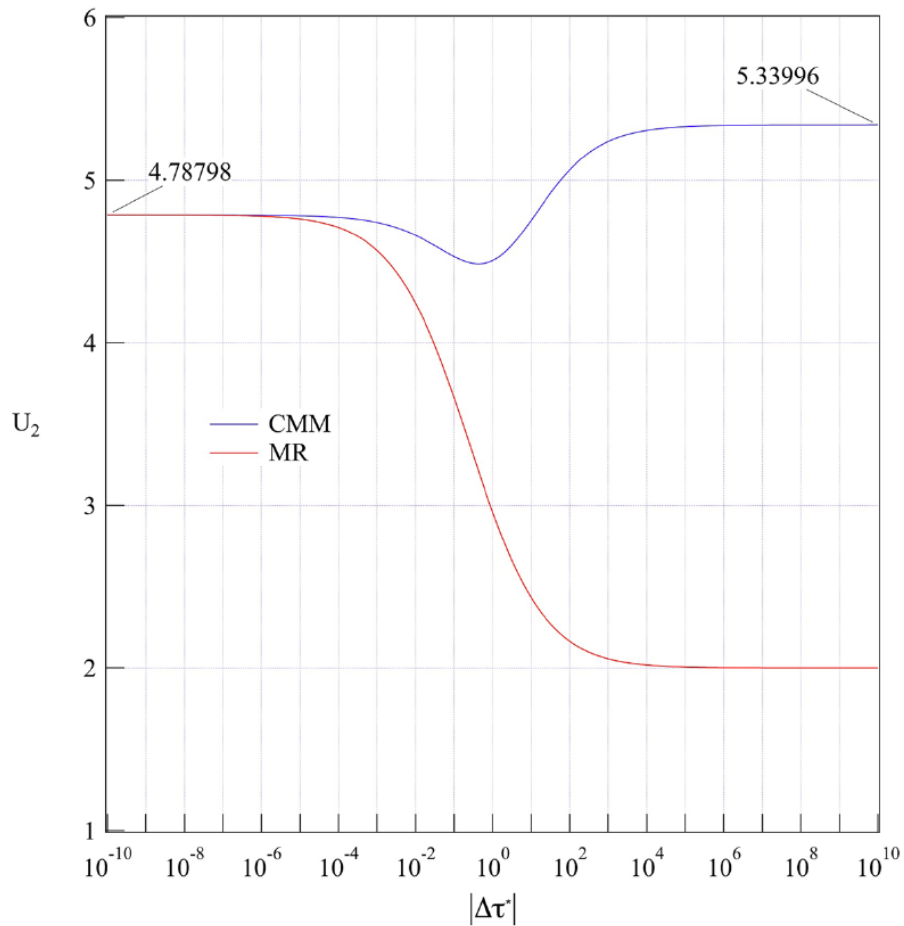


Fig. 6 Universal amplitude ratio U_2 calculated from intrinsic CMM (blue curve labelled CMM) and ideal CMM (red curve labelled MR), the latter being obtained (see text) from the corresponding MR crossover functions

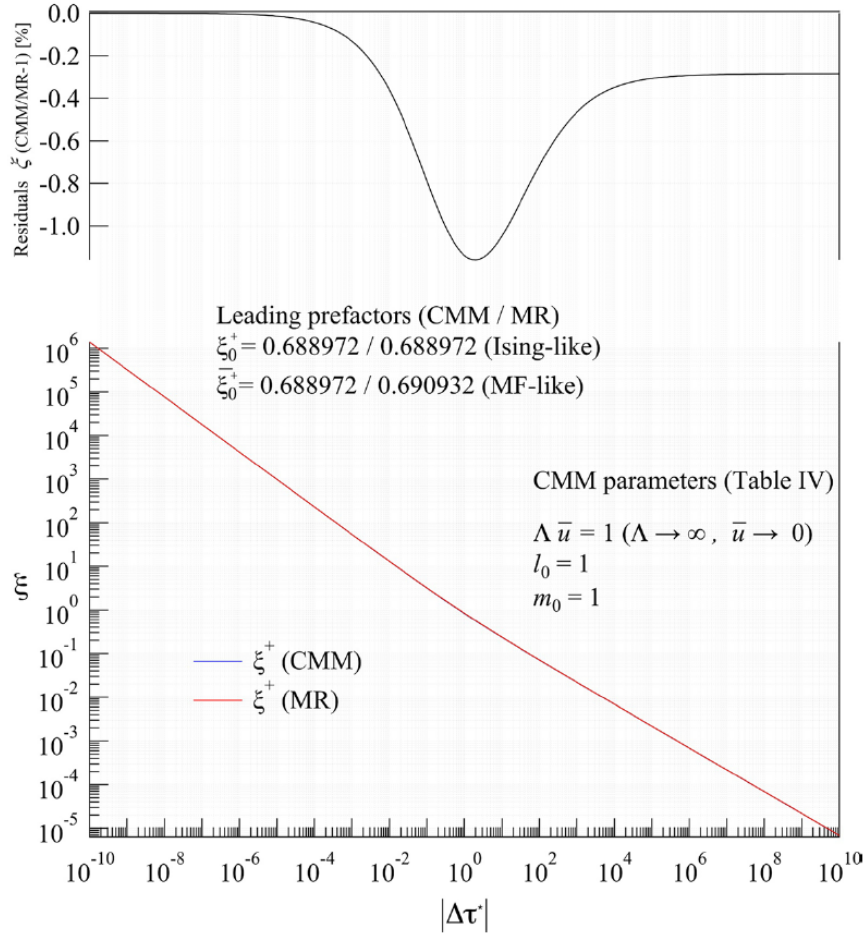


Fig. 7 Same as Fig 1 for the correlation length case ξ^+ in the homogeneous domain

$\Delta\tilde{\rho}_{LV} = \frac{\rho_L - \rho_V}{2\rho_c}$ (where ρ_L and ρ_V are the liquid and vapor density of the two coexisting phases) from $\Delta\tilde{\rho}$ can be found in Refs. [18, 22] for example.

An essential complementary result is given by the Fig. 9 where are illustrated the complete behavior of the universal combination $Q^+ = \alpha(\Delta\tau^*)^2 C^+ (\xi^{*,+})^d$, which confirms the correct account for common critical scaling between thermodynamics and correlation properties (see text and Eqs. A12 and (A13) in Appendix A).

As in Fig. 5, the Ising limit $Q^+ = 0.01961673$ (see Table 3) is not reached at $\Delta\tau^* = 10^{-10}$ (where $Q_e^+ = 0.01777$), certainly due to the similar large confluent effect observed on the combination between the correlation length and specific heat properties calculated from the MR crossover functions above T_c .

As a main common observation on each related figure for χ^+ , C^+ , ξ^+ , χ^- , C^- , and m , the exact agreement between intrinsic CMM and ideal CMM for the asymptotic Ising limit $|\Delta\tau^*| \ll 1$ with Ising universal exponents γ , α , ν , and β as a slope, and prefactor \mathfrak{Z}_χ^+ , \mathfrak{Z}_C^+ , \mathfrak{Z}_ξ^+ , \mathfrak{Z}_χ^- , \mathfrak{Z}_C^- , and \mathfrak{Z}_M as an amplitude, respectively, is clearly evidenced by the zero value limit of the residuals. In a similar manner, the intrinsic non matching of the two models for the mean-field limit $|\Delta\tau^*| \gg 1$, is illustrated by

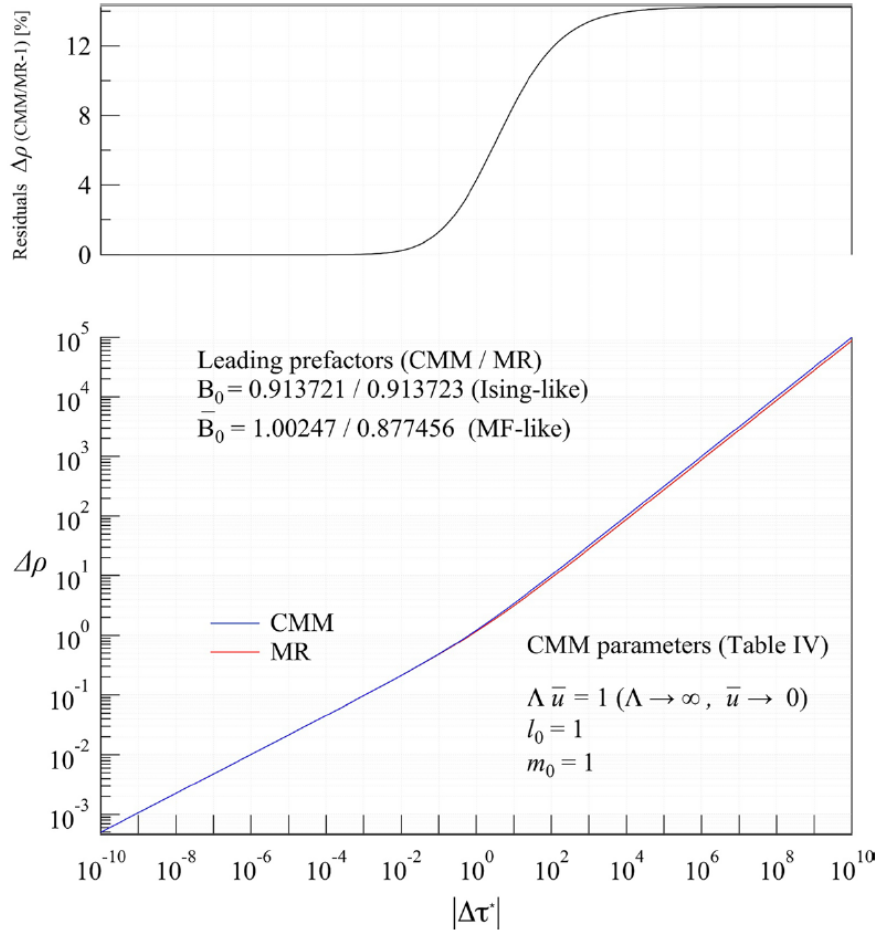


Fig. 8 Same as Fig 2 for the order parameter case $m^* = \Delta\rho^*$ in the non-homogeneous domain and reference to Table II of Ref. [17]

distinct mean-field prefactor amplitudes $\overline{3}_\chi^+ \neq \overline{3}_{m,\chi}^+$, $\overline{3}_C^+ \neq \overline{3}_{m,C}^+$, $\overline{3}_\xi^+ \neq \overline{3}_{m,\xi}^+$, $\overline{3}_\chi^- \neq \overline{3}_{m,\chi}^-$, $\overline{3}_C^- \neq \overline{3}_{m,C}^-$, and $\overline{3}_M \neq \overline{3}_{m,M}$ and associated finite limit value of each residual.

Complementary comparisons can be observed from the bottom part of Figs. 10, 11, 12, 13, 14, 15, where are illustrated the corresponding behavior of each related effective exponent $\pi_{e,P} = \text{sign}\left(\frac{d \ln P^l}{d \ln \Delta\tau^*}\right)$ [41] as a function of $\Delta\tau^*$. sign means the \pm choice to make positive the exponent value (as in Table 2). In the top part of each figure are illustrated the related residuals $r\pi_{e,P} \% = 100 \times \left[\frac{\pi_{e,P,CMM}}{\pi_{e,P,MR}} - 1 \right]$ for all the exponents, except for α where the absolute difference $\delta\alpha_e = 1000 \times [\alpha_{e,CMM} - \alpha_{e,MR}]$ is more appropriate to the values of this effective exponent. Such residuals behaviors appear in conformity with the infinite-cutoff approximation, for both Ising-like and classical asymptotic limits. In the case of susceptibility effective exponent γ_e in the homogeneous domain, in Fig. 10, the comparison with CPM model is also shown.

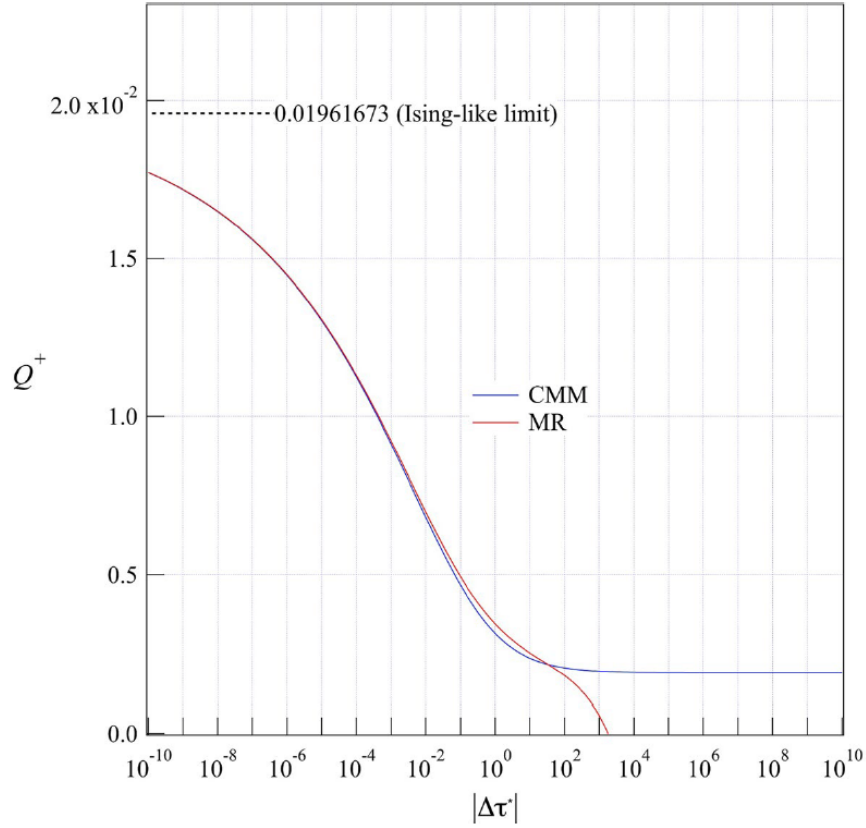


Fig. 9 Universal amplitude ratio Q^+ calculated from intrinsic CMM (blue curve labelled CMM) and ideal CMM (red curve labelled MR), the latter being obtained (see text) from the corresponding MR crossover functions

Finally, the largest temperature range, typically $10^{-10} \leq \Delta\tau^* \leq 10^{10}$, is convenient to show the exact agreement of intrinsic CMM with the Ising-like asymptotic behavior of the MR crossover functions for $\Delta\tau^* \rightarrow 0$ and to magnify the corresponding residuals for, either the non matching amplitude differences, or the perfect exponent matching in the classical limit $\Delta\tau^* \rightarrow \infty$.

The essential practical interest results in the straightforward determination of the Ising-like applicability range of intrinsic CMM. Indeed, the temperature-like range of the PAD where the three-scaling-factor universality of Ising-like systems is accounted for by the MR crossover functions reads $t \leq \mathcal{L}_{\text{PAD,MR}}^{\text{Ising}} \simeq 1.9 \times 10^{-6}$ [17]. The equivalent $\Delta\tau^*$ range for CMM writes

$$\Delta\tau^* \leq \mathcal{L}_{\text{PAD,CMM}}^{\text{Ising}} = \frac{\mathcal{L}_{\text{PAD,MR}}^{\text{Ising}}}{\Theta_m} \simeq 6 \times 10^{-4} \quad (83)$$

Then, for any one component fluid, the practical order of magnitude for the extended asymptotic range $\Delta\tau^* \leq \mathcal{L}_{\text{EAD,CMM}}^{\text{Ising}} \simeq 5 \times 10^{-2}$ can be estimated for CMM from the

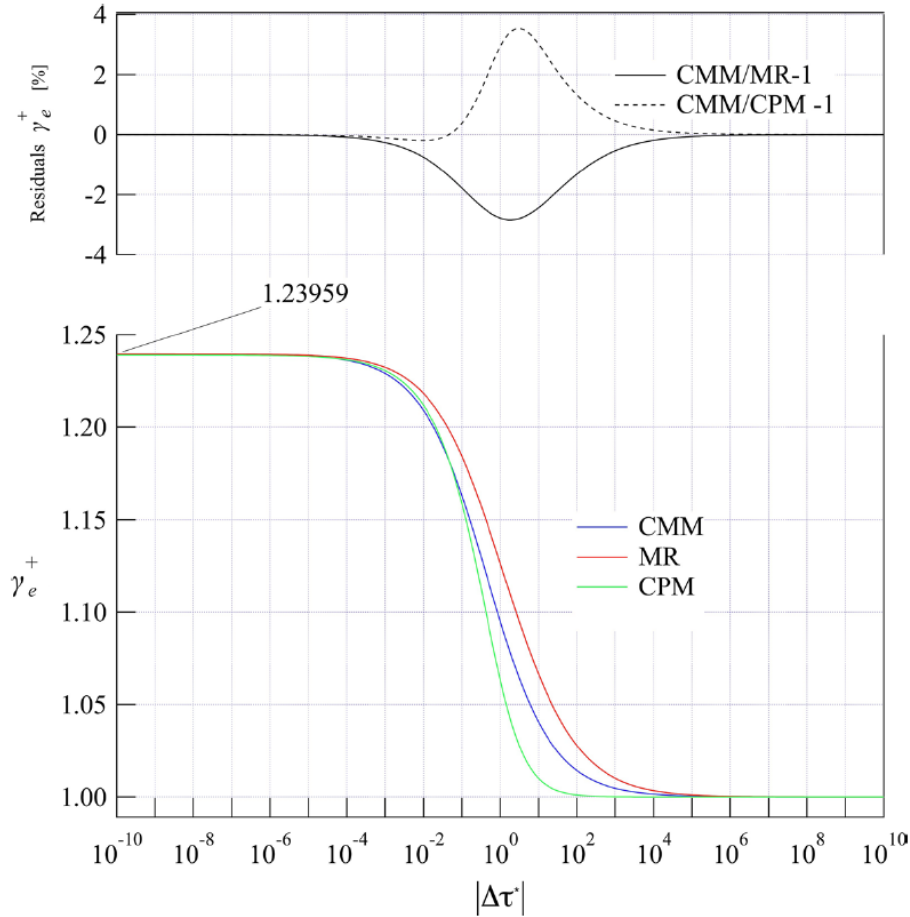


Fig. 10 Comparison of susceptibility effective exponent γ_e in the homogeneous domain calculated from intrinsic CMM (blue curve labelled CMM), CPM (green curve labelled CPM), and ideal CMM (red curve labelled MR), the latter being obtained (see text) from the corresponding MR crossover function χ^* (see Table I of Ref. [17]). The Ising value $\gamma = 1.2395935$ (see line) is given in Table 2. The respective residuals, $\chi_{\gamma_e}^* \% = 100 \times \left[\frac{\gamma_e^{(CMM)}}{\gamma_{re}^{(MR)}} - 1 \right]$ (solid line) and $= 100 \times \left[\frac{\gamma_e^{(CMM)}}{\gamma_{re}^{(CPM)}} - 1 \right]$ (dashed line) are shown in the top part plot

well defined MR applicability range observed in [22], on the basis of the xenon case [18] used as a reference simple fluid.

4 Conclusion

A new extended set of parametric equations to describe the crossover master model (CMM) of the equation of state and the correlation length of any simple fluid near its liquid–gas critical point was defined. The intrinsic parametric form of CMM involves 10 universal thermodynamic parameters and 6 universal correlation parameters unequivocally estimated from 16 universal amplitude ratios and amplitude combinations. Among these 16 parameters, only the values of b^2 and w_0 , obtained from $\frac{A_1^+}{A_1^-}$ (see Eqs. 37 and 68) and Z_C^+ (see Eqs. 35 and 70) respec-

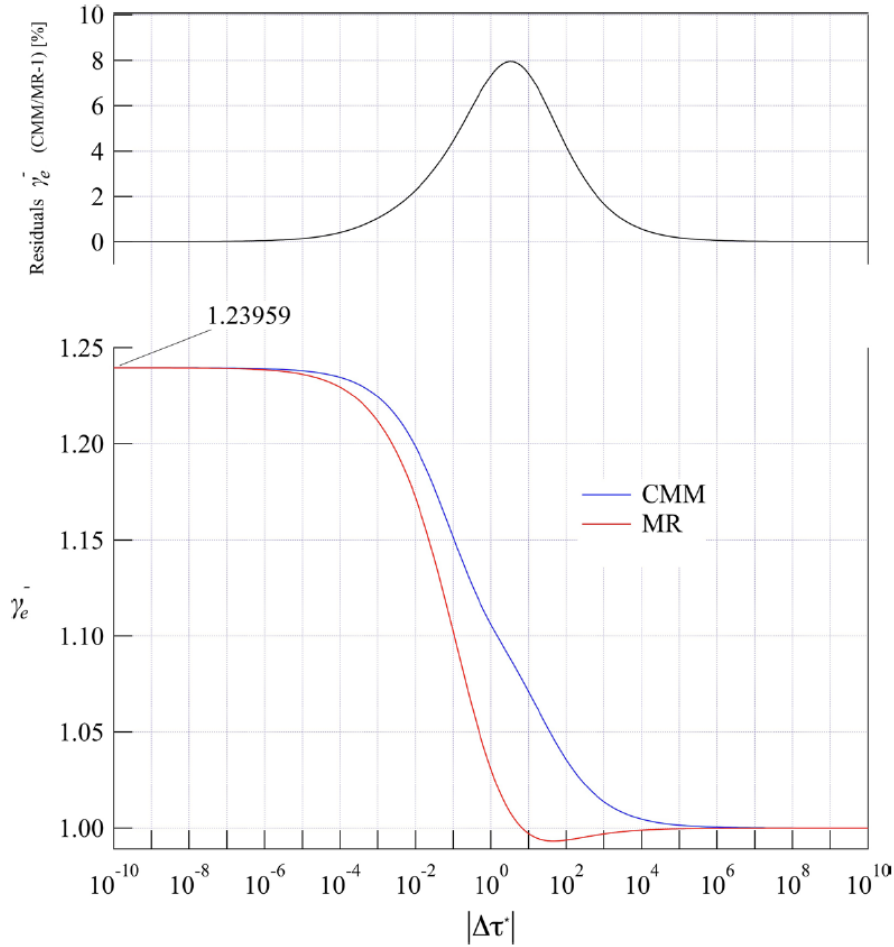


Fig. 11 Same as Fig 10 (except for CPM comparison) for the non homogeneous domain. The Ising value $\gamma = 1.2395935$ (see line) is given in Table 2

tively, are readily independent. The actual amplitude checking concerns a set of 26 selected amplitudes given in Table 1. The corresponding set of 26 universal prefactors is made of 10 Ising-like leading prefactors, 7 first-order confluent correction prefactors, and 9 mean-field-like prefactors, related by 20 universal amplitude ratios and amplitude combinations.

Therefore, two Ising-like leading prefactors, (\mathfrak{Z}_χ^+ and \mathfrak{Z}_C^+), and one first-order confluent correction prefactor, ($\mathfrak{Z}_\chi^{1,+}$), are really independent on CMM, leading to the mean-field description characterized by only two related mean-field-like prefactors, ($\overline{\mathfrak{Z}_\chi^+}$ and $\overline{\mathfrak{Z}_C^-}$), when the value $\overline{\mathfrak{Z}_C^+} = \overline{A_0^+} = 0$ is postulated.

The construction of the ideal parametric form of CMM using these 16 universal parameters and the three additional master scaling factors \mathbb{L}_m , Θ_m , and Ψ_m reveals the quasi-perfect matching of the Ising-like critical limit, including the first-order of the confluent corrections to scaling. Indeed, the estimations of 10 master Ising-like leading amplitudes match exactly their corresponding master MR values, in conformity with the Ising-like universal features of the MR scheme. The amplitude and the extension of the non-perfect matching at the first-order confluent

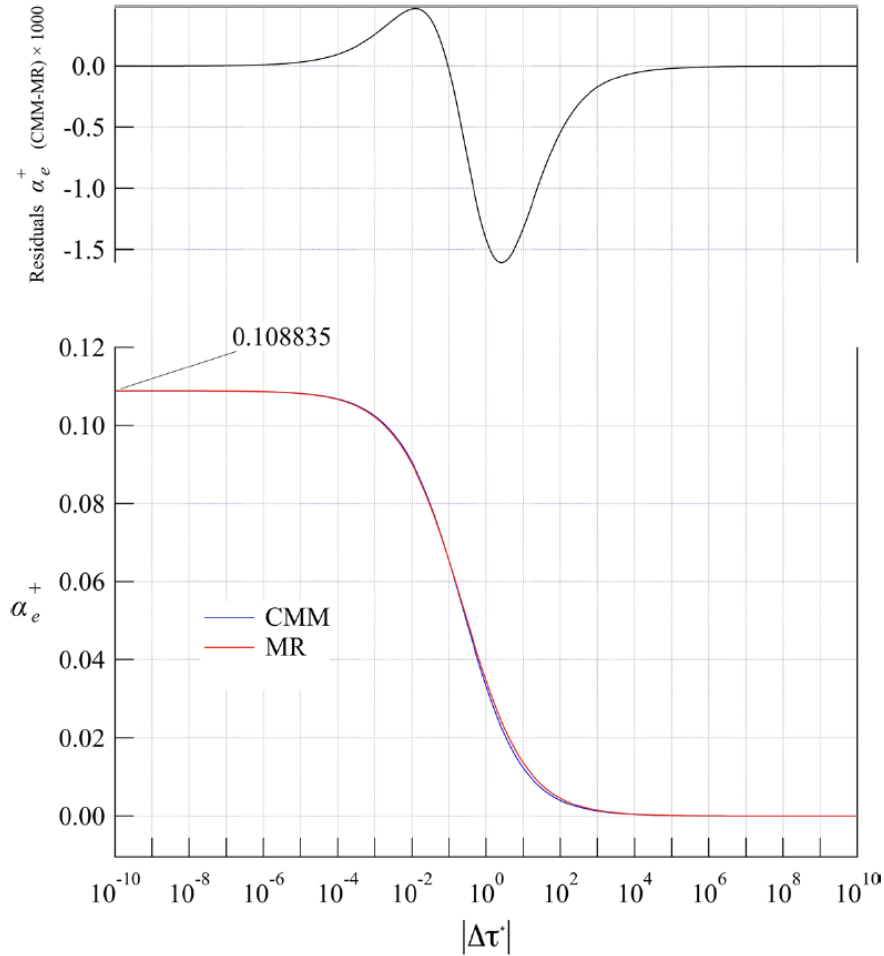


Fig. 12 Same as Fig 10 (except for CPM comparison) for the heat capacity exponent case α_e in the homogeneous domain, except the absolute difference $\delta\alpha_e = 1000 \times [\alpha_e^+(\text{CMM}) - \alpha_e^+(\text{MR})]$ shown in the top part plot. The Ising value $\alpha = 0.1088375$ (see line) is given in Table 2

corrections-to-scaling are well defined when they occur only in the restricted case of the heat capacity at constant volume above and below T_c . In addition, among the estimations of 7 master confluent amplitudes, only 3 match exactly with their master MR values. The residuals for the non-exact intrinsic confluent amplitudes are in the 3% range.

The resulting construction of the mean-field classical limit of the intrinsic CMM distinguishes from the one of the ideal CMM. Indeed, the estimations of 9 master mean-field leading amplitudes depart from their corresponding values obtained from the classical limit of the MR crossover functions, especially in the case of the isothermal susceptibility. However, 5 among the 6 mean-field features of the corresponding amplitude combinations are exactly recovered (with $\overline{c_q^+} = 1$ fixed), and then only one ($\overline{U_2}$) departs from its mean-field value. Despite this single main difference, it is then essential to note that the number of physical independent

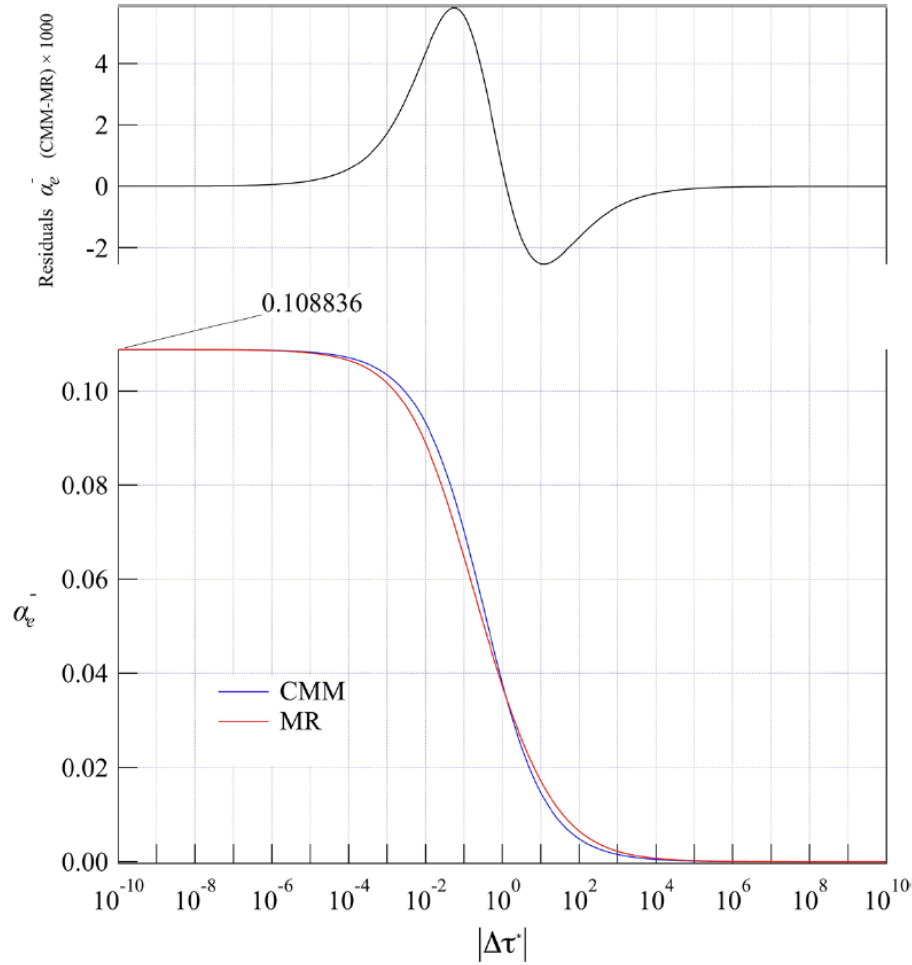


Fig. 13 Same as Fig 12 for the heat capacity exponent case α_e in the non homogeneous domain. The Ising value $\alpha = 0.1088375$ (see line) is given in Table 2

parameters remains well controlled. The mean-field classical limit results in conformity with the basic three-term Landau expansion (adding then one postulated constraint $\overline{A}_0^+ = 0$ for the specific heat case above T_c and consequently two additional amplitude combinations $\overline{U}_0 = \frac{\overline{A}_0^+}{\overline{A}_0^-} = 0$ and $\overline{Q}^+ = \overline{A}_0^+ (\xi_0^{*,+})^d = 0$).

As a main conclusive remark, the present work, added to the ones of Refs. [18, 22, 34], gives a complete analysis of the expected singular description of any simple fluids. Reference [18] starts from the xenon case to define the needed master constants of the simple fluid subclass [18]. Then, Ref. [22] illustrates the uniqueness nature of the Ising-like crossover parameter within a well-defined finite asymptotic range. Reference [34] provides the equivalence between any Ising-like crossover descriptions using three fluid dependent parameters. Finally, the present determinations of the ideal and intrinsic CMM close the parametric description of the complete e.o.s. in conformity with the analytic one of the MR crossover functions [17] calculated for the $\mathcal{O}(1)$ universality class defined by $\{d = 3, n = 1\}$. As a more interesting practical result, the singular

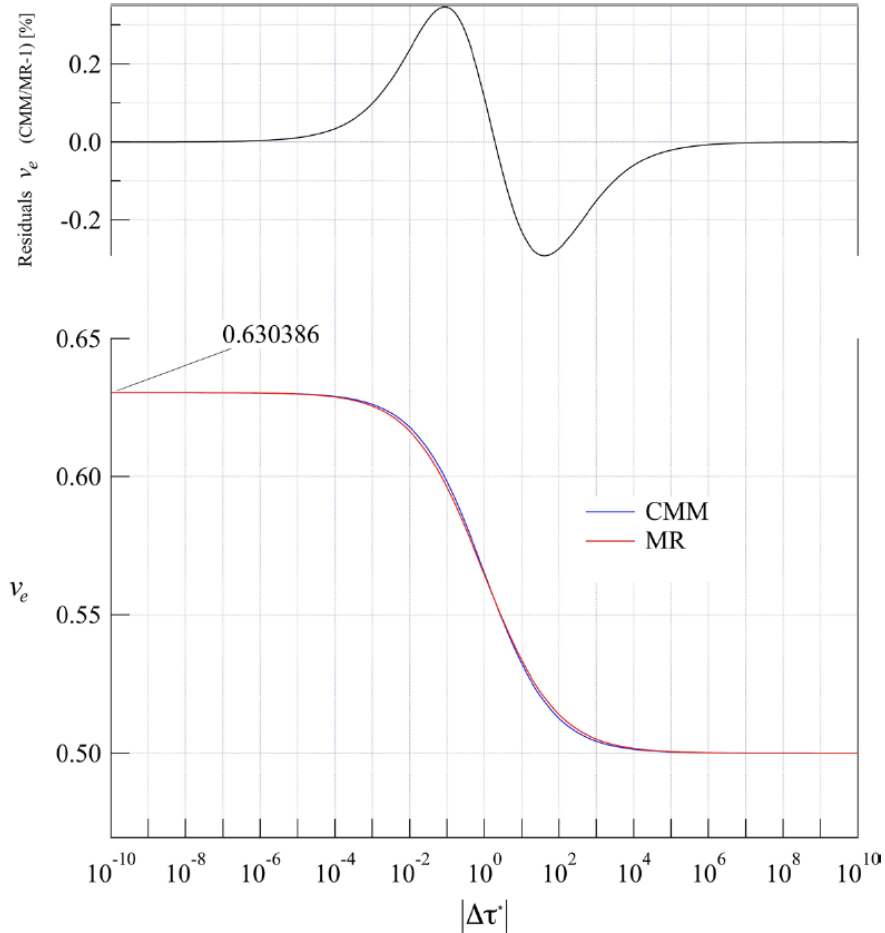


Fig. 14 Same as Fig 10 (except for CPM comparison) for the correlation length exponent case v_e in the homogeneous domain. The Ising value $\nu = 0.6303875$ (see line) is given in Table 2

description of any simple fluid can then be made in a well defined finite asymptotic domain whatever the considered three parameters crossover model only using the four generalized critical coordinates of its liquid–gas critical point, as initially suggested in Refs. [14, 42, 43].

Appendix A: MR-Like Characteristic Parameters of the CMM

The main objective of this Appendix A is to provide an unambiguous analytical determination of the 16 universal parameters of Table 4 involved by the CMM parametric forms of the e.o.s.. Despite the irreducible defaults of the resulting intrinsic CMM, this closed determination then permits to use, for such a similar determination, any theoretical crossover behavior calculated along the renormalized trajectory of the $O(1)$ symmetric $(\Phi^2)^2$ field theory [4]. The first Section of this Appendix A provides the needed normed quantities that are defined in conformity with the use of Σ_0 as a dimensionless energy density reference (see previous section 2.2.). The second Section provides the

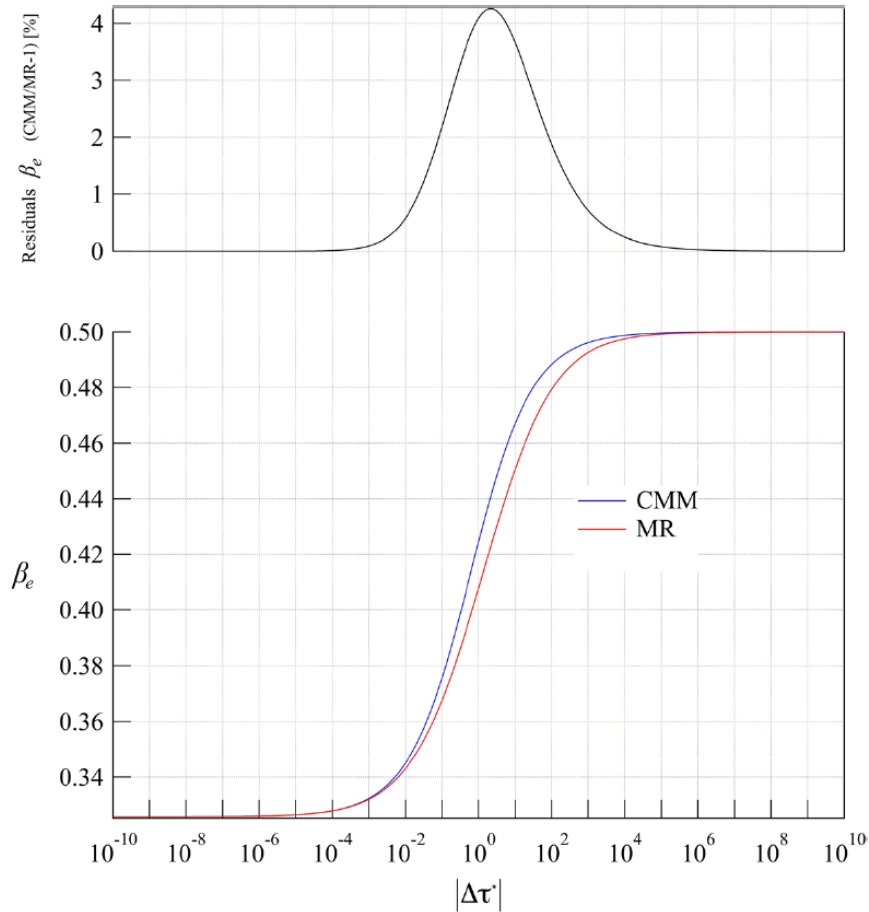


Fig. 15 Same as Fig 10 (except for CPM comparison) for the order parameter exponent case β in the non-homogeneous domain

76 successive steps of the unequivocal process to determine these 16 normed universal parameters reported in column 5 of Table 4.

Normed Universal Prefactors for the Universal Thermodynamic and Correlation Properties

The CMM construction only considers normed quantities using as dimensionless references, Σ_0 for the thermodynamics functions, $(\Sigma_0)^{-\frac{1}{3}}$ for the correlation functions (to be in conformity with the Q^+ universality), and consequently, $(\Sigma_0)^{-\frac{5}{3}}$ for the correlation angular functions. The non-universal nature of the physical system is then suppressed using the following four universal parametric equations

$$k(\theta) = 1 - b^2\theta^2, \quad (\text{A1})$$

$$l^*(\theta) = \frac{l(\theta)}{l_0} = \frac{\tilde{l}(\theta)}{\tilde{l}_0} \quad (\text{A2})$$

$$= \theta(1 - \theta^2)(1 + d\theta^2 + e\theta^4 + f\theta^6)$$

$$w^*(\theta) = \frac{w(\theta)}{m_0 l_0 \Sigma_0} = \frac{\tilde{w}(\theta)}{\tilde{m}_0 \tilde{l}_0 \Sigma_0} \quad (\text{A3})$$

$$= (w_0^* + w_1^* \theta^2 + w_2^* \theta^4 + w_3^* \theta^6 + w_4^* \theta^8 + w_5^* \theta^{10})$$

$$a_r(\theta, Y_1) = \frac{a(\vartheta, Y_1)}{(m_0)^{-\frac{5}{3}} (l_0)^{\frac{1}{3}} (\Sigma_0)^{-\frac{5}{3}}} = \frac{\tilde{a}(\vartheta, Y_1)}{(\tilde{m}_0)^{-\frac{5}{3}} (\tilde{l}_0)^{\frac{1}{3}} (\Sigma_0)^{-\frac{5}{3}}} \quad (\text{A4})$$

$$= (a_{r0} + a_{r1} \theta^2 + a_{r2} \theta^4) Y_1 + (a_{r0}^* + a_{r1}^* \theta^2 + a_{r2}^* \theta^4) (1 - Y_1)$$

All the 16 unknown parameters can be distinguished in a set $\{b^2, d, e, f\}$ of 4 parameters independent of Σ_0 and a set $\{w_i^*, a_{rj}, a_{rj}^*\}$ (with $i = \{0, 5\}$ and $j = \{0, 2\}$), of 12 normed parameters with reference to Σ_0 . Accordingly, the 5 normed and 2 reduced quantities of practical interest read as follows

$$w_0^* = \frac{\tilde{w}(0)}{\tilde{m}_0 \tilde{l}_0} \frac{1}{\Sigma_0} = \frac{w_0}{\Sigma_0} \quad (\text{A5})$$

$$w_1^* = \frac{1}{2} \frac{\tilde{w}''(0)}{\tilde{m}_0 \tilde{l}_0} \frac{1}{\Sigma_0} = \frac{w_1}{\Sigma_0} \quad (\text{A6})$$

$$\Sigma_1^* = \frac{\Sigma_1}{\Sigma_0} = 2 \sum_{j=0}^{j=5} j w_j^* \quad (\text{A7})$$

$$\Sigma_2^* = \frac{\Sigma_2}{\Sigma_0} = 2 \sum_{j=0}^{j=5} j(2j-1) w_j^* \quad (\text{A8})$$

$$S_0^* = \frac{S_0}{\Sigma_0} = \sum_{j=0}^{j=5} w_j^* \left(\frac{1}{b^2}\right)^j \quad (\text{A9})$$

$$L_0^* = -\frac{l'(1)}{2l_0} = -\frac{\tilde{l}'(1)}{2\tilde{l}_0} = 1 + d + e + f \quad (\text{A10})$$

$$f = L_0^* - 1 - d - e \quad (\text{A11})$$

When b^2 is used as entry data in Eq. A1, the knowledge of w_0^* (Eq. A5) and w_1^* (Eq. A6) close the normed description of respectively the heat capacity above and

below T_c and the isothermal susceptibility above T_c (see Eqs. 33 to 36 and Eqs. 39, 40). The parameter set $\{w_0^*, w_1^*, \Sigma_0^* = 1, \Sigma_1^*, \Sigma_2^*, S_0^*\}$ of Eqs. A5 to A9 closes the universal parametric form of Eq. A3. In addition, L_0^* of Eq. A10 provides access to one parameter among $\{d, e, f\}$, as for example f of Eq. A11. The parameter set $\{d, e, L_0^*\}$ is then equivalent to the $\{d, e, f\}$ set and finally closes the estimation of universal parametric Eq. A1.

Similarly, Eqs. 30, 31 and 32 can be now rescaled to induce the following normed prefactors

$$\frac{P_0^l}{f_{P,\text{Ising}}^l(m_0, l_0)} \left(\frac{1}{\Sigma_0} \right)^{n_p} = \mathfrak{Z}_P^{*,l} \quad (\text{A12})$$

$$\frac{\overline{P_0^l}}{f_{P,\text{mf}}^l(\tilde{m}_0, \tilde{l}_0)} \left(\frac{1}{\Sigma_0} \right)^{n_p} = \overline{\mathfrak{Z}_P^{*,l}} \quad (\text{A13})$$

where $n_p = 1$ for the thermodynamic properties and $n_p = -\frac{1}{3}$ for the correlation lengths. The normed prefactors are labeled with the added superscript $*$. They are related to Eqs. A5 to A11 through the different values of the normed angular functions for $\vartheta = \left\{ 0, 1, \left| \frac{1}{b} \right| \right\}$ (also labeled with the added superscript $*$). They are obtained from the corresponding angular functions given in Appendix A of Ref. [24]. We note that the Σ_0 dependence in the angular correction-to-scaling functions disappears introducing the normed parameters. The values of the first-order confluent correction prefactors of Eqs. 31 are then unchanged.

Analysis of Ref. [24] is complemented by 26 universal normed prefactors defined in column 2 of Table 6, where, as previously in Table 5, part (a) corresponds to the Ising-like leading prefactors (using Eqs. A(18) to A(23) of Ref. [24]), part (b) corresponds to the first-order confluent prefactors obtained from Eqs. A(45) to A(49) of Ref. [24] and part (c) corresponds to the mean-field leading prefactors (using Eqs. (4.45) to (4.49) of Ref. [24]).

The normed equation number (with added label n) corresponds to the equation number given in Ref. [24] (see column 3). In column 2, some universal prefactors are given explicitly when they appear in simple forms of exponent combinations (as in lines 11(*) and 13(e2)), or parameters b^2 and w_0^* of Eq. A5 (as in lines 1n(e3+), 2n(e3-), and 12). More complex implicit forms express their functional dependence in some auxiliary universal quantities of Eqs (A7) to (A11). In the $\{d, e, f\}$ -dependent case, the prefactors are given in the functional forms illustrating their L_0^* dependence in place of f dependence. Therefore, when the universal values of the exponent are fixed to their MR and MF values (see Table 2), the hierarchical calculations of these universal parameters can be performed using the MR-Ising-like and mean-field-like ratios and combinations of Table 3.

A special mention concerns the ordering case of a_{ij} and a_{ij}^* involved in Eq. A4. We recall first Eqs. (5.168) and (5.169) of the Agayan's dissertation,

Table 6 Column 2: Parametric definition of the normed universal prefactors (see text) involved in the determination of 26 physical quantities reported in Table 1. (a) 10 Ising-like leading prefactors, (b) 7 first-order confluent prefactors, (c) 9 mean-field-like prefactors. Column 3: Corresponding normed equation (with added label n) given in Ref. [24]. Column 4: line-step number of Table 8 given in Appendix A where is performed the unequivocal determination of each normed prefactor. Column 1: ordering number (added label n refers to a normed prefactor (see Table 5 and text))

Line number	Table 5	Equation number [24]	Line-step number Table 8
(a)	Ising-like normed prefactors		
1n(e3+)	$\frac{A_0^+}{m_0} \frac{1}{\Sigma_0} = \mathfrak{3}_C^{*+} = q_2^*(0) = -(2 - \alpha)(1 - \alpha)w_0^*$	(A18)n	11
2n(e3-)	$\frac{A_0^-}{m_0} \frac{1}{\Sigma_0} = \mathfrak{3}_C^{*-} = (b^2 - 1)^\alpha q_2^*(1) = -(b^2 - 1)^{\alpha-2} (2 - \alpha)(1 - \alpha)\Sigma_1^*(b^2)$	(A19)n	8
3n(e4)	$\frac{\Gamma_0^+}{m_0} \frac{1}{(l_0)^{-1} \Sigma_0} = \mathfrak{3}_\chi^{*+} = q_1^*(0) = -2[(2 - \alpha)b^2 w_0^* + w_1^*(b^2, L_0^*)]$	(A21)n	27
4n	$\frac{\Gamma_0^-}{m_0} \frac{1}{(l_0)^{-1} \Sigma_0} = \mathfrak{3}_\chi^{*-} = (b^2 - 1)^\gamma q_1^*(1) = \mathfrak{3}_\chi^{*-} [b^2, \Sigma_1^*(b^2), \Sigma_2^*(b^2, L_0^*, d, e)]$	(A22)n	56
5n	$\frac{B_0}{m_0} \frac{1}{\Sigma_0} = \mathfrak{3}_M^* = (b^2 - 1)^{-\beta} m_1^*(1) = (b^2 - 1)^{-\beta} \left[\frac{(2-\alpha)b^2}{1-b^2} - \frac{\Sigma_1^*}{2} \right] (L_0^*)^{-1}$	(A20)n	28
6n	$\frac{D_0}{(m_0)^{-\frac{1}{3}} (l_0)^{-\frac{1}{3}} \Sigma_0} = \mathfrak{3}_H^* = l^* \left(\frac{1}{b} \right) \left[m_1^* \left(\frac{1}{b} \right) \right]^{-\delta} = \mathfrak{3}_H^* [b^2, S_{0,1}^*(b^2, L_0^*, d, e)]$	(A23)n	57
7n	$\frac{\Gamma_0^c}{m_0} \frac{1}{(l_0)^{-\frac{1}{2}} \Sigma_0} = \mathfrak{3}_\chi^{*c} = \frac{1}{\delta} (\mathfrak{3}_H^*)^{-\delta}$		58
8n	$\frac{\xi_0^+}{(m_0)^{-\frac{1}{3}} (l_0)^{-\frac{1}{3}} \Sigma_0} = \mathfrak{3}_\xi^{*+} = \sqrt{\mathfrak{3}_\chi^{*+} a_{r0}}$		31
9n	$\frac{\xi_0^-}{(m_0)^{-\frac{1}{3}} (l_0)^{-\frac{1}{3}} \Sigma_0} = \mathfrak{3}_\xi^{*-} = \sqrt{\mathfrak{3}_\chi^{*-} (a_{r0} + a_{r1} + a_{r2})} (b^2 - 1)^{\eta\nu}$		70
10n	$\frac{\xi_0^c}{(m_0)^{-\frac{1}{3}} (l_0)^{-\frac{1}{3}} \Sigma_0} = \mathfrak{3}_\xi^{*c} = \sqrt{\mathfrak{3}_\chi^{*c} (a_{r0} + a_{r1} \frac{1}{b^2} + a_{r2} \frac{1}{b^4})} \left[l^* \left(\frac{1}{b} \right) \right]^{\frac{\eta\nu}{\beta\delta}}$		71

Table 6 (continued)

Line number	Equation number [24]	Line-step number Table 8
(b) Confluent correction-to-scaling prefactors		
11(e1+)	(A45)	1
	$\frac{A_1^+}{g^{-\Delta_\chi(1-\bar{\nu})}} = 3_C^{1,+} = 2\alpha + 2\Delta q_{2,1}(0) = 2\alpha \left[1 + \Delta \frac{(3+\Delta-\alpha)}{(1-\alpha)(2-\alpha)} \right]$	
12(e1-)	(A46)	7
	$\frac{A_1^-}{g^{-\Delta_\chi(1-\bar{\nu})}} = 3_C^{1,-} = (b^2 - 1)^{-\Delta} [2\alpha + 2\Delta q_{2,1}(1)] = (b^2 - 1)^{-\Delta} 2\alpha \left[1 + \Delta \frac{(3+\Delta-\alpha)}{(1-\alpha)(2-\alpha)} \right]$	
13(e2)	(A48)	2
	$\frac{\Gamma_1^+}{g^{-\Delta_\chi(1-\bar{\nu})}} = 3_\chi^{1,+} = 2(\gamma - 1) + 2\Delta q_{1,1}(0) = 2(\gamma - 1)$	
14	(A49)	55
	$\frac{\Gamma_1^-}{g^{-\Delta_\chi(1-\bar{\nu})}} = 3_\chi^{1,-} = 3_\chi^{1,-} \left[b^2, \Sigma_1^*(b^2), \Sigma_{2,CC}^*(b^2, L_0^*, d, e) \right]$	
15	(A47)	17
	$\frac{B_1}{g^{-\Delta_\chi(1-\bar{\nu})}} = 3_M^1 = \frac{1-2\beta+2\Delta m_{1,1}(0)}{(b^2-1)^\Delta} = \left[1 - 2\beta + 2\Delta \frac{-2\alpha b^2}{-2(2-\alpha)b^2 - (1-b^2)\Sigma_1^*} \right] (b^2 - 1)^\Delta$	
16		62
	$\frac{\xi_1^+}{g^{-\Delta_\chi(1-\bar{\nu})}} = 3_\xi^{1,+} = 3_\chi^{1,+} \left(\frac{\xi_1^+}{\Gamma_1^+} \right)$	
17		63
	$\frac{\xi_1^-}{g^{-\Delta_\chi(1-\bar{\nu})}} = 3_\xi^{1,-} = 3_\chi^{1,-} \left(\frac{\xi_1^-}{\Gamma_1^-} \right)$	
(c) mean-field-like normed prefactors		
18n	(4.49)n	15
	$\frac{\Delta C_V g^{-\alpha}}{\bar{n}_{b_0}} \frac{1}{\Sigma_0} = \overline{\Delta C_V} = \overline{3_C^{*-}} = 2w_0^* - \frac{2}{(1-b^2)^2}$	
19n	(4.47)n	29
	$\frac{\overline{\Gamma_0} g^{1-\gamma}}{\bar{n}_{b_0} (f_0)^{-1} \Sigma_0} = \overline{3_\chi^{*+}} = \overline{q_1^*}(0) = -2[2b^2 w_0^* + w_1^*(b^2, L_0^*)]$	
20n	(4.47)n	59
	$\frac{\overline{\Gamma_0} g^{1-\gamma}}{\bar{n}_{b_0} (f_0)^{-1} \Sigma_0} = \overline{3_\chi^{*-}} = (b^2 - 1) \overline{q_1^*}(1) = \overline{3_\chi^{*-}} \left[b^2, \Sigma_1^*(b^2), \Sigma_{2,MF}^*(b^2, L_0^*, d, e) \right]$	
21n	(4.46)n	30
	$\frac{\overline{B_0} g^{\mu-\frac{1}{2}}}{\bar{n}_{b_0} \Sigma_0} = \overline{3_M^*} = (b^2 - 1)^{-\frac{1}{2}} \overline{m_1^*}(1) = (b^2 - 1)^{-\frac{1}{2}} \left[\frac{2b^2}{1-b^2} - \frac{\Sigma_1^*}{2} \right] (L_0^*)^{-1}$	

Table 6 (continued)

Line number	Equation number [24]	Line-step number Table 8
22n	$\frac{D_0 g^{-\frac{2-\nu}{3}}}{(\tilde{m}_0)^{-\frac{2-\nu}{3}} (\Sigma_0)^{-3}} \frac{1}{\Sigma_0} = \overline{3}_H^* = \tilde{r}^* \left(\left \frac{1}{b} \right \right) \left[m_1^* \left(\left \frac{1}{b} \right \right) \right]^{-3} = \overline{3}_H^* \left[b^2, S_{0,MF}^* (b^2, L_0^*, d, e) \right]$	(4.48)n 60
23n	$\frac{\overline{I}_0^c g^{-\alpha}}{\tilde{m}_0 (t_0)^{-\frac{1}{3}}} \frac{1}{\Sigma_0} = \overline{3}_\chi^{*,c} = \frac{1}{3} (\overline{3}_H^*)^{-3}$	61
24n	$\frac{\overline{\Sigma}_0^c g^{\frac{1-\nu}{3}}}{(\tilde{m}_0 t_0)^{-\frac{1}{3}} (\Sigma_0)^{-3}} \frac{1}{\Sigma_0} = \overline{3}_\xi^{*,+} = \sqrt{\overline{3}_\chi^{*,+} a_{r0}^*}$	32
25n	$\frac{\overline{\Sigma}_0^c g^{\frac{1-\nu}{3}}}{(\tilde{m}_0 t_0)^{-\frac{1}{3}} (\Sigma_0)^{-3}} \frac{1}{\Sigma_0} = \overline{3}_\xi^{*,-} = \sqrt{\overline{3}_\chi^{*,-} (a_{r0}^* + a_{r1}^*)}$	76
26n	$\frac{\overline{\Sigma}_0^c g^{\frac{1-\nu}{3}}}{(\tilde{m}_0 t_0)^{-\frac{1}{3}} (\Sigma_0)^{-3}} \frac{1}{\Sigma_0} = \overline{3}_\xi^{*,c} = \sqrt{\overline{3}_\chi^{*,c} (a_{r0}^* + a_{r1}^* \frac{1}{b^2} + a_{r2}^* \frac{1}{b^4})}$	77

Table 7 Column 2: Normed functional forms of auxiliary parameters. Column 3: line-step number of Tables 8 in Appendix A where is performed the unequivocal determination of the normed auxiliary parameter

	auxiliary parameters and their functional forms with $\Sigma_0^* = 1$	Line-step number
1	$\mathfrak{Z}_{B_{cr}}^* = -2w_0^*$	13
2	$c_q^+ = \left[\frac{2Q^+}{v(1-\alpha)(2-\alpha)} \right]^{\frac{1}{3}}$	24
3	$\Sigma_1^*(b^2) = \frac{2b^2}{b^2-1} \left[2 - \alpha - \frac{2\alpha\Delta}{(B_1/\Gamma_1^+) \mathfrak{Z}_\gamma^{1+} (b^2-1)^{\Delta-1+2\beta}} \right]$	16
4	$\tilde{w}^{in}(0) \propto w_{1, \text{Ising}}^* [R_C, b^2, \Sigma_1^*(b^2), L_0^*]$	21
5	$\tilde{w}^{in}(0) \propto w_{1, \text{MF}}^* [\overline{R}_C, b^2, \Sigma_1^*(b^2), L_0^*]$	21
6	$L_0^* = L_0^*(b^2, w_0^*, \Sigma_1^*)$	20
7	$S_0^* = S_{0, \text{Ising}}^{*,c} [R_\gamma, b^2, \Sigma_1^*(b^2), d, e]$	47
8	$S_0^* = S_{0, \text{MF}}^{*,c} [\overline{U}^c, b^2, \Sigma_1^*(b^2), d, e]$	47
9	$\Sigma_2^* = \Sigma_{2, \text{Ising}}^* [U_2, b^2, \Sigma_1^*(b^2), L_0^*, d, e]$	46
10	$\Sigma_2^* = \Sigma_{2, \text{CC}}^* [(\Gamma_1^+/\Gamma_1^-), b^2, \Sigma_1^*(b^2), L_0^*, d, e]$	46
11	$\Sigma_2^* = \Sigma_{2, \text{MF}}^* [\overline{U}_2, b^2, \Sigma_1^*(b^2), L_0^*, d, e]$	48
12	$\Sigma_0^* = \sum_{j=0}^{j=5} w_j^*$	53
13	$K_1 = (U_2/U_\xi^2)(b^2-1)^{\eta\nu}$	65
14	$K_c = \left\{ q_1^*(0) \left[q_1^* \left(\left \frac{1}{b} \right \right) \right]^{-1} \right\}^{\frac{-\eta}{2-\eta}} [Q_2]^{\frac{2}{2-\eta}}$	66
15	$\overline{K}_1 = (\overline{U}_\xi^-)^2 \overline{U}_2 \neq 1$	71
16	$\overline{K}_c = \left(\frac{\overline{\xi}_0^c / \overline{\xi}_0^+}{\overline{\xi}_0^+} \right)^2 \left(\frac{\overline{\Gamma}_0^+ / \overline{\Gamma}_0^c}{\overline{\Gamma}_0^+} \right) = 1$	72

$$\frac{(\xi_0^+)^2}{\Gamma_0^+} = a(0) \quad \frac{(\xi_0^-)^2}{\Gamma_0^-} = a(1) |k(1)|^{\eta\nu} \quad \frac{(\xi_0^c)^2}{\Gamma_0^c} = a \left(\left| \frac{1}{b} \right| \right) \left| l \left(\left| \frac{1}{b} \right| \right) \right|^{\frac{\eta\nu}{\beta\delta}}$$

complemented by the similar equations from the mean-field classical limit,

$$\frac{(\overline{\xi}_0^+)^2}{\overline{\Gamma}_0^+} = a^\star(0) \quad \frac{(\overline{\xi}_0^-)^2}{\overline{\Gamma}_0^-} = a^\star(1) \quad \frac{(\overline{\xi}_0^c)^2}{\overline{\Gamma}_0^c} = a^\star \left(\left| \frac{1}{b} \right| \right)$$

This special mention refers to the control of Q^+ , U_ξ , and Q_2 for the Ising-like critical limit ($Y_1 \rightarrow 1$), or, \overline{U}_ξ (with $(\overline{U}_\xi^-)^2 \equiv \overline{U}_2$) and \overline{Q}_2 for the mean-field-like classical limit ($Y_1 \rightarrow 0$).

Ising-Like Limit

The parameter a_0 can be estimated from $a_0 = \frac{1}{q_1(0)} \left[\frac{Q^+}{aq_2(0)} \right]^{\frac{2}{3}}$ (see Eq. 5.173(n), Agayan thesis), which then leads to the values of a_{r0} and $\mathfrak{Z}_\xi^{*,+}$ in agreement with Q^+ . Simultaneously, we note that our CMM value $c_q^+ = 0.3330078$ (line (2) in Table 7), obtained from the MR results, differs from the CPM one $c_q^+ = 0.3286$ (see Eq. 5.191, Agayan thesis). Subsequently, in the Agayan dissertation, the parameter a_1 was calculated to recover only the universal combination U_ξ . In our present extended Eq. A4, the a_{r1}, a_{r2} pair increases the control to the U_ξ, Q_2 pair. Indeed, it is now possible to calculate the two quantities $K_1 = \frac{U_2}{U_\xi^2} \times \frac{1}{(b^2-1)^{-\eta}}$ and $K_c = \left[\frac{q_1^*(0)}{q_1^*\left(\frac{1}{b}\right)} \right]^{\frac{-\eta}{2-\eta}} [Q_2]^{\frac{2}{2-\eta}}$, that induce the values of $a_{r1}, a_{r2}, \mathfrak{Z}_\xi^{*-},$ and $\mathfrak{Z}_\xi^{*,c}$. Finally, the complete Ising-like triad $\{a_{ri}\}$ induces the unequivocal control of the Ising-like combinations triad $\{Q^+, U_\xi, Q_2\}$. However, as already noted by Agayan, the universal combination U_2 can be never explicitly controlled through K_1 . Such a result confirms a needed alternative way to account for the MR value of U_2 (see below).

Mean-Field-Like Limit

The estimation of the mean-field-like triad a_{ri}^* follows in a similar manner. The parameter a_{r0}^* can be estimated from the normed Eq. 5.186(n) of the Agayan's thesis, using now $c_q^+ = 1$, and noting that $\mathfrak{Z}_{B_{cr}}^* = -2w_0^*$. Subsequent estimation of $\overline{\mathfrak{Z}_\xi^{*,+}}$ occurs also in similar agreement. From the Agayan's CPM, the non-zero value of a_{r1}^* only provides the control of $\overline{U_\xi}$ and gives thus a measure of the non-exact mean-field value of $\overline{U_2}$ since a_{r1}^* only vanishes when $\left(\overline{U_\xi}\right)^2 \equiv \overline{U_2}$, identically. However, we note that the mean-field like universal combination $\overline{Q_2}$ (see line 20(e) in Table (3)) plays a similar role to Q_2 when the $\{a_{r1}^*, a_{r2}^*\}$ pair is accounted for in the classical limit ($Y_1 \rightarrow 0$) of Eq. 12. Consequently, the estimations of $\overline{D_0^c} = \frac{\tilde{l}\left(\frac{1}{b}\right)}{\left[\overline{m_1}\left(\frac{1}{b}\right)\right]^3}$ and

$\overline{\Gamma_0^c} = \tilde{q}_1\left(\frac{1}{b}, 0\right) \times \left[\tilde{l}\left(\frac{1}{b}, 0\right)\right]^{1-\frac{1}{3}}$ to validate the relation $\overline{\Gamma_0^c} = \frac{1}{3\left(\overline{D_0^c}\right)^{\frac{1}{3}}}$, show that the

two quantities $\overline{K_1} = \left(\overline{U_\xi}\right)^{-2} \times \frac{\overline{\Gamma_0^+}}{\overline{\Gamma_0^c}}$ and $\overline{K_c} = \left(\frac{\overline{\xi_0^c}}{\overline{\xi_0^+}}\right)^2 \frac{\overline{\Gamma_0^+}}{\overline{\Gamma_0^c}}$ (equal to unity for the ideal mean-field behavior), can be used to obtain the two equations $a_{r1}^* = a_{r0}^* \times \frac{(\overline{K_c}-1)b^4 - (\overline{K_1}-1)}{b^2-1}$ and $a_{r2}^* = a_{r0}^* \times \frac{(\overline{K_c}-1)b^4 - (\overline{K_1}-1)b^2}{1-b^2}$ (which replace

Table 8 Hierarchical determination step by step (column 1) of the normed, universal prefactors, universal parameters, and universal auxiliary quantities involved in the CMM correlation functions

	normed prefactor order (Table 6)	universal combination order (Table 3)	universal parameter order (Table 4)	Prefactors/Parameters	reduced value
1	11(e1+)			$\mathfrak{Z}_C^{1,+} = 2\alpha \left[1 + \Delta \frac{(3+\Delta-\alpha)}{(1-\alpha)(2-\alpha)} \right]$	0.437624
2	13(e2)			$\mathfrak{Z}_X^{1,+} \equiv \mathfrak{Z}_{m,x}^{1,+} = 2(\gamma-1)$	0.479187
3		10(i)		$\frac{\mathfrak{Z}_C^{1,+}}{\mathfrak{Z}_X^{1,+}} = \frac{\alpha}{(\gamma-1)} \left[1 + \frac{\Delta(3+\Delta-\alpha)}{(1-\alpha)(2-\alpha)} \right] = \frac{A_1^+}{\Gamma_1^+}$	0.913263
4		9(e)-(e1)	1	$b^2 = 1 + \left(\frac{A_1^+}{A_1} \right)^{\frac{1}{\Delta}}$ (8)	2.44726
5				$q_2^*(1) = -(2-\alpha)(1-\alpha)(b^2-1)^{-2} \Sigma_0^*$	
6				$\overline{q_2^*(1)} = -2(b^2-1)^{-2} \Sigma_0^*$	
7	12(e1-)			$\mathfrak{Z}_C^{1,-} = (b^2-1)^{-\Delta} \mathfrak{Z}_C^{1,+}$	0.363351
8	2n(e3-)			$\mathfrak{Z}_C^{*,-} = -(b^2-1)^{\alpha-2} (2-\alpha)(1-\alpha)$	-0.837654
9		1(e)	2n	$w_0^* = U_0(b^2-1)^{\alpha-2}$ (8)	0.266804
10				$q_2^*(0) = -(2-\alpha)(1-\alpha)w_0^*$	
11	1n(e3+)			$\mathfrak{Z}_C^{*,+} = -(2-\alpha)(1-\alpha)w_0^*$	-0.449654
12				$\overline{q_2^*(0)} = -2w_0^*$	
13				$\mathfrak{Z}_{B_r}^* = -2w_0^*$	-0.533608
14				$\overline{\mathfrak{Z}_C^{*,+}} = -2w_0^* - \mathfrak{Z}_{B_r}^*$	0
15	18n			$\overline{\mathfrak{Z}_C^{*,-}} = \overline{\Delta C_V^*} = 2w_0^* - \frac{2}{(1-b^2)^2}$	-0.421242
16	12(e)	12(e)	18n	$\Sigma_1^* = \frac{2b^2}{b^2-1} \left[2 - \alpha - \frac{2\alpha\Delta}{\Gamma_1^+ \mathfrak{Z}_X^{1,+} (b^2-1)^\Delta - 1 + 2\beta} \right]$	4.23203

$$\frac{B_{\sigma,\sigma'}}{m_{q_0}} = \frac{B_{\sigma}}{m_{q_0}} = \mathfrak{Z}_{B_r}^*$$

$$A_0^+ = 0 \left(\frac{A_1^+}{A_0^+} = \overline{U_0} \equiv 0 \right)$$

Table 8 (continued)

	normed prefactor order (Table 6)	universal combination order (Table 3)	universal parameter order (Table 4)	Prefactors/Parameters	reduced value
17	15			$\mathfrak{Z}_M^1 = \frac{1-2\beta+2\Delta}{(b^2-1)^\Delta} \frac{-2\alpha b^2}{-2(2-\alpha)b^2-(1-b^2)^{\frac{2-\alpha}{2}}} = \frac{B_1}{\Gamma_1} \mathfrak{Z}_\chi^{1,+}$	0.431268
18	3(e)			$w_{1,\text{Ising}}^* [R_C, b^2, \Sigma_1^*(b^2), L_0^*] \propto \tilde{w}^{**}(0)_{\text{Ising}}$	
19	16(e)			$w_{1,\text{MF}}^* [\overline{R}_C, b^2, \Sigma_1^*(b^2), L_0^*] \propto \tilde{w}^{**}(0)_{\text{MF}}$	
20		21n		$L_0^* = L_0^*(b^2, w_0^*, \Sigma_1^*)$	1.28654
21		3n		$w_1^* = w_{1,\text{Ising}}^* = w_{1,\text{MF}}^*$	0.908857
22				$q_1^*(0) = -2[(2-\alpha)b^2 w_0^* + w_1^*]$	
23				$\overline{q_1^*(0)} = -2[2b^2 w_0^* + w_1^*]$	
24	7(e)			$c_q^+ = \left[\frac{2Q^+}{v(1-\alpha)(2-\alpha)} \right]^{\frac{1}{3}}$	0.3330078
25		11		$a_{r0} = \frac{1}{q_1^*(0)} \left[\frac{Q^+}{\alpha q_2^*(0)} \right]^{\frac{2}{3}}$	-0.833916
26		14		$a_{r0}^* = \frac{a_{r0}}{c_q} \times \frac{q_1^*(0)}{q_1^*(0)}$	-0.684650
27	3n(e4)			$\mathfrak{Z}_\chi^{*+} = -2[(2-\alpha)b^2 w_0^* + w_1^*]$	-0.651915
28	5n			$\mathfrak{Z}_M^* = (b^2 - 1)^{-\beta} \left[\frac{(2-\alpha)b^2}{1-b^2} - \frac{\Sigma_1^*}{2} \right] (L_0^*)^{-1}$	-0.745496
29	19n			$\overline{\mathfrak{Z}_\chi^{*+}} = -2[2b^2 w_0^* + w_1^*]$	-0.794044
30	21n			$\overline{\mathfrak{Z}_M^*} = (b^2 - 1)^{-\frac{1}{2}} \left[\frac{2b^2}{1-b^2} - \frac{\Sigma_1^*}{2} \right] (L_0^*)^{-1}$	-0.817906
31				$\mathfrak{Z}_\xi^{*+} = \sqrt{\mathfrak{Z}_\chi^{*+} a_{r0}}$	-0.737321
32				$\overline{\mathfrak{Z}_\xi^{*+}} = \sqrt{\overline{\mathfrak{Z}_\chi^{*+}} a_{r0}^*}$	-0.737321

Table 8 (continued)

	normed prefactor order (Table 6)	universal combination order (Table 3)	universal parameter order (Table 4)	Prefactors/Parameters	reduced value
33				$f(x, y) = L_0^* - 1 - x - y$	
34	4(e)			$S_0^* = S_{0, \text{Ising}}^{*,c} [R_\chi, b^2, \Sigma_1^*(b^2), x, y]$	
35	17(e)			$S_0^* = S_{0, \text{MF}}^{*,c} [\overline{U}^c, b^2, \Sigma_1^*(b^2), x, y]$	
36			$S_{0, \text{Ising}}^{*,c} = S_{0, \text{MF}}^{*,c}$	$Y_{0, \text{Ising+MF}}^* = -0.258794 - 3.44726x$	$C1(x, y)$
37	2(e)			$\Sigma_{2, \text{Ising}}^* (U_2, x, y)$	
38	11(e)			$\Sigma_{2, \text{CC}}^* \left[\frac{\Gamma_1^+}{\Gamma_1^-}, b^2, \Sigma_1^*(b^2), L_0^*, x, y \right]$	
39	15(e)			$\Sigma_{2, \text{MF}}^* (\overline{U}_2, x, y)$	
40			$\Sigma_{2, \text{Ising}}^* = \Sigma_{2, \text{CC}}^*$	$Y_{\Sigma_{2, \text{Ising+CC}}^*} = 2 \times (0.7887367 - x)$	$C2a(x, y)$
41			$\Sigma_{2, \text{Ising}}^* = \Sigma_{2, \text{MF}}^*$	$Y_{\Sigma_{2, \text{Ising+MF}}^*} = 2 \times (0.2923855 - x)$	$C2b(x, y)$
42			$\Sigma_{2, \text{CC}}^* = \Sigma_{2, \text{MF}}^*$	$Y_{\Sigma_{2, \text{CC+MF}}^*} = 2 \times (0.4456573 - x)$	$C2c(x, y)$
43			$C1(x, y) = C2a(x, y)$	$d = x_0$	-1.2687866
44				$e = y_0 = y(x_0)$	4.11505
45				$f = L_0^* - 1 - x_0 - y_0$	2.55972
46				$\Sigma_2^* = \Sigma_{2, \text{IsingorCC}}^* (x_0, y_0)$	19.8117
47				$S_0^* = S_{0, \text{IsingorMF}}^{*,c} (x_0, y_0)$	0.1647
48	15(i)		$\Sigma_{2, \text{MF}}^* (d, e)$	$\neq \Sigma_2^*$	20.9477
49				$w_5^* (\Sigma_1^*, w_1^*, \Sigma_2^*, \delta_0^*)$	2.27629
50				$w_4^* (\Sigma_1^*, w_1^*, \Sigma_2^*, \delta_0^*)$	-6.005
51				$w_3^* (\Sigma_1^*, w_1^*, \Sigma_2^*, \delta_0^*)$	4.9219
52				$w_2^* (\Sigma_1^*, w_1^*, \Sigma_2^*, \delta_0^*)$	0.448865

Table 8 (continued)

	normed prefactor order (Table 6)	universal combination order (Table 3)	universal parameter order (Table 4)	Prefactors/Parameters	reduced value
53	12n		17n	$\sum_{j=0}^{j=5} w_j^*$	1
54		2(e), 9(e)-(e1)		$q_1^*(1) = (U_2)^{-1} \left(\frac{A_1^+}{A_1^-} \right)^{-\frac{1}{\Delta}} q_1^*(0)$	
55	14			$3_{\chi}^{*1,-} = \left(\frac{A_1^+}{A_1^-} \right)^{-1} 3_{\chi}^{*1,+}$	-2.264394
56	4n			$3_{\chi}^{*-} = (b^2 - 1)^{-\gamma} q_1^*(1)$	0.136146
57	6n			3_H	-7.97256
58	7n			3_{χ}^{*c}	-0.135105
59	20n			$\overline{3_{\chi}^{*-}}$	-0.148687
60	22n			$\overline{3_H}$	-1.88256
61	23n			$\overline{3_{\chi}^{*c}}$	-0.269958
62	16			$3_{\xi}^{*1,+} = 3_{\chi}^{*1,+} \left(\frac{\xi^+}{\Gamma^+} \right)$	
63	17			$3_{\xi}^{*1,-} = 3_{\xi}^{*1,+} \left(\frac{\xi^+}{\xi^-} \right)^{-1}$	
64				$q_1^* \left(\left \frac{1}{b} \right \right)$	
65				$l^* \left(\left \frac{1}{b} \right \right) = l^* \left(\left \frac{1}{b} \right , d, e \right)$	
66				$K_1 = \frac{U_2}{U_1^2} \times \frac{1}{(b^2-1)^{-\eta}}$	
67				$K_c = \left[\frac{q_1^{*(0)}}{q_1^* \left(\left \frac{1}{b} \right \right)} \right]^{2-\eta} [Q_2]^{2-\eta}$	

Table 8 (continued)

	normed prefactor order (Table 6)	universal combination order (Table 3)	universal parameter order (Table 4)	Prefactors/Parameters	reduced value
68			12	$a_{r1} = a_{r0} \times \frac{(K_c-1)b^{k_1} - (K_1-1)}{b^{k_2-1}}$	-0.406224
69			13	$a_{r2} = a_{r0} \times \frac{(K_c-1)b^{k_1} - (K_1-1)b^2}{b^{k_2-1}}$	-0.208818
70	9n			\mathfrak{Z}_ξ^{*-}	-0.376184
71	10n			\mathfrak{Z}_ξ^{*c}	0.358701
72				$\overline{K}_1 = (\overline{U}_\xi)^2 \overline{U}_2 \neq 1$	
73				$\overline{K}_c = \left(\frac{\overline{\kappa}_c}{\overline{\kappa}_0}\right)^2 \frac{\Gamma_0^-}{\Gamma_0}$	1
74			15	$a_{r1}^* = a_{r0}^* \left[\frac{\overline{U}_2}{(\overline{U}_\xi)^2} - 1 \right]$	0.0185851
75			16	$a_{r2}^* = a_{r0}^* \left(\frac{b^2}{b^{k_2-1}} \right) \left[\frac{\overline{U}_2}{(\overline{U}_\xi)^2} - 1 \right]$	-0.0438793
76	25n			\mathfrak{Z}_ξ^{*-}	
77	26n			\mathfrak{Z}_ξ^{*c}	

Column 1: line-step number. Column 2: normed prefactor order listed in column 1 of Table (6). Column 3: amplitude combination order listed in column 1 of Table (3) (added label n recalls for account of their normed form). Column 4: normed parameter order listed in column 6 of Table (4). Column 5: constraint accounted for in the current line-step. The both independent universal parameters are labelled with (\otimes) . Column 6: resulting normed functional form from reference to Σ_0^* . Column 7: resulting numerical value when available (with $\Sigma_0^* = 1$)

Eq. 5.187(n) of Agayan thesis). Adding the practical simplification where $\overline{Q_2} = 1 \equiv \overline{K_c}$ finally provides the values of a_{r1}^* , a_{r2}^* , $\overline{\mathfrak{Z}_\xi^{*-}}$, and $\overline{\mathfrak{Z}_\xi^{*c}}$.

Therefore, the classical triad $\{a_{ri}^*\}$ induces the unequivocal control of the Ising-like triad $\{c_q^+, \overline{U_\xi}, \overline{Q_2}\}$. Nevertheless, the non-zero values of a_{r1}^* and a_{r2}^* are measuring the non-exact mean-field value of $\overline{U_2}$ since $\overline{K_1}$ differs from the unity only if $\overline{U_2} = \frac{\overline{\Gamma_0^+}}{\overline{\Gamma_0^-}} \neq 2$ (that is precisely the case in intrinsic CMM as in the Agayan's CPM). We also note that the classical $\overline{U_2}$ -value is never controlled from the classical triad $\{a_{ri}^*\}$, a similar situation to the unchecked U_2 -value from the Ising-like triad $\{a_{ri}\}$.

Closed Estimation of the Normed Universal Prefactors

Ordering estimation of the quantities involved in our unequivocal process are listed in columns 6 and 7 from successive line-steps 1 to 77 of Tables 8. Columns 1, 2, and 3 give the ordering account for the normed prefactors (see Table 6), their corresponding universal ratios or combinations (from Table 3), and the resulting universal normed parameters (from Table 5), respectively. Column 4 reports the references used to support the estimation or the functional condition controlled at this step.

The series of equations start from our initial choices of the three first-order confluent amplitudes A_1^\pm and Γ_1^+ to define previous Eqs. 68 to 72. The prefactors $\mathfrak{Z}_C^{1,+}$, $\mathfrak{Z}_\chi^{1,+}$ and their ratio, are only dependent on the α, γ, Δ exponent values and definitively departs from their MR value. Selecting then the MR condition $\frac{A_1^+}{A_1^-} = 1.20386$ (see line 9(e)-(e1) in Table 3) leads to $b^2 = 2.44726$. Here is eliminated an alternative way where another selected MR ratio value $\frac{A_1^-}{\Gamma_1^+} = 0.782374$ (see line $\frac{10}{9}$ (i) in Table 3) can produce a different value $b_{C\chi}^2 = 2.36$. However the impact of this latter value remains on the same order of magnitude ($\simeq 3\%$) for intrinsic versus ideal CMM. Moreover, the uncertainties in the determination of the first-order confluent amplitudes along the critical isochore remain larger than 3% (see the $\Gamma_1^+ (\equiv a_\chi^{1,+})$ case as typical example reported in Table 4 of Ref. [18]).

The most essential point remains that only one among the 7 first-order confluent amplitudes is independent in intrinsic CMM accordingly to the MR results, while 5 among the 7 take same ideal CMM value. De facto, when $b^2 = 2.44726$ (line-step 4), all the quantities of line-steps 5 to 17 (with $\Sigma_0^* = 1$), which are either α, γ, Δ -dependent or $\{d, e, f\}$ non-dependent, can be estimated. In particular, that includes $\mathfrak{Z}_{B_{cr}}^*$ (line-step 13) and $\overline{\mathfrak{Z}_C^{*-}}$ (line-step 15).

At the line step 17, we note that the unequivocal determination of the three (with 2 normed) parameters b^2, w_0^*, Σ_1^* of Table 4 complies with the MR values of the three universal ratios $\frac{A_1^+}{A_1^-}, U_0, \frac{B_1}{\Gamma_1^+}$. At the opposite, the values of three universal ratios $\frac{A_1^+}{\Gamma_1^+}, \frac{A_1^+}{B_1}, \frac{A_1^-}{B_1}$ depart intrinsically from their corresponding MR value.

The line-steps from 18 to 32 provide the additional estimations of L_0^* and w_1^* , starting from the selected condition $\tilde{w}^{\cdot}(0)_{\text{Ising}} = \tilde{w}^{\cdot}(0)_{\text{MF}}$ between the auxiliary functional forms reported in lines 2 and 3 of Table 7. Accounting in addition for the MR value of Q^+ and for fixed value $\overline{c}_q^+ = 1$ (as in CPM), all the prefactors defined in line-steps 26 to 32 are then back obtained.

The final approach consists in introducing in line-step 33 a function $f(x, y)$ of the two variables x and y , which replace the two parameters d and e , respectively, and to then write all the remaining unknown quantities in terms of x and y . The needed first closure equation $C1(x, y)$ is thus provided considering in line-step 36 the identity $S_{0,\text{Ising}}^{*,c} = S_{0,\text{MF}}^{*,c}$ between Ising and mean-field auxiliary functional forms (see lines 5 and 6 of Table 7), which then account for two additional normed amplitude combinations R_χ and $\overline{U^c} = \overline{R_\chi}$ (see lines 4(e) and 17(e) of Table 3). This analytical process provides two respective values of the same parameter S_0^* , whose equality involves a single solution $y(x) = y(S_0^*)$ (see line-step 36 in Table 8). In a similar manner, the needed second closure equation is based on the identity between two respective values of the same functional (Ising-like, confluent, and mean-field like) parameters Σ_2^* , only dependent on x, y . This second closure equation is not unique since the three different functional forms of Σ_2^* (see lines 7, 8, and 9 of Table 7) account for three universal normed combinations $U_2, \frac{\Gamma_1^+}{\Gamma_1},$ and $\overline{U_2}$ (see lines 2(e), 11(e), and 15(i) in Table 3), respectively. The corresponding results are not compatible with a single common solution for $y(\Sigma_2^*)$, as illustrated by the equations reported in column 6 line-steps 40 to 42, and labelled $C2a(x, y), C2b(x, y), C2c(x, y)$ in column 7 of Table 8. To maintain asymptotic Ising-like coherence in the construction process the selected second equation is then Eq. $C2a(x, y)$, which accounts for U_2 and $\frac{\Gamma_1^+}{\Gamma_1}$, simultaneously. Such a choice provides the needed alternative way mentioned just above (section “**Ising-Like Limit**”) to account for U_2 . However the alternative choice that maintains the control of $\overline{U_2}$ in place of $\frac{\Gamma_1^+}{\Gamma_1}$ will be estimated in a forthcoming work for comparison on the crossover effect. The common single solution x_0 of the condition $C1(x, y) = C2a(x, y)$ (see line-step 43) provides the estimation of $d = x_0, e = y(x_0)$ and then in return $f = L_0^* - 1 - x_0 - y_0, \Sigma_2^* = \Sigma_{2,\text{IsingorCC}}^*(x_0, y_0)$ and $S_{0,\text{IsingorMF}}^{*,c}(x_0, y_0)$. We mention the resulting difference $\Sigma_{2,\text{MF}}^*(d, e) \neq \Sigma_2^*$ of $\simeq 5.6\%$ (line step 48). The parameter set $\{w_2^*, w_3^*, w_4^*, w_5^*\}$ (lines steps 49 to 52) involved in Eq. 15 results from the parameter set $\{w_1^*, \Sigma_1^*, \Sigma_2^*, S_0^*\}$, leading to the successive knowledge of the complete remaining line-steps until 77, except the ones where parametric formulation from CPM, or related MR values, are here not available. We note that the construction of Eq. A4 is now fully achieved.

Obviously, the complete identification between the MR crossover functions and intrinsic CMM needs to reintroduce the reference sum Σ_0 throughout, either $w_0^* = \frac{w_0}{\Sigma_0} = 0.266804$ combined to Eq. 70, or $b^2 = 2.44726$ combined to Eq. 71. As mentioned previously, w_0^* and b^2 are both universal independent parameters in Table 8, as well as w_0 and b^2 are both universal independent parameters in

Table 4, indicated by the label \otimes . As previously expected, w_0 , or Σ_0 , defines the single energy density reference of dimensionless CMM, above or below T_c .

The final important remark concerning the above unequivocal process is its possible use whatever the exact numerical results of the universal exponents and universal combinations provided by any theoretical crossover functions calculated for the $N = 1$ -vector model of three-dimensional (3D) Ising like systems and/or the $O(1)$ symmetric $(\Phi^2)^2$ Field Theory (FT) framework [4]. We also note a recent work by Dohm [44] suggesting that the Ising universality class includes not only isotropic fluids but also weakly anisotropic Φ^4 model. This equation-of-state modeling effort could also apply to such weakly anisotropic magnetic systems provided that the isotropic correlation length is replaced by the mean correlation length of the anisotropic system. In such a case, the model could be tested with numerical simulations of isotropic Ising models in an external magnetic field.

Acknowledgements YG and CL acknowledge Fabien Palencia for his support and contribution using Mathematica. We thank CNES and CNRS agencies, through the GdR MFA, for supporting the research at ICMCB, and also NASA for supporting the research of IH at Jet Propulsion Laboratory and California Institute of Technology.

Author Contributions Y.G., C.L., and I.H. wrote the main manuscript text. Y.G. prepared the Tables and I.H. prepared the figures. All authors reviewed the manuscript.

Funding The research at ICMCB was supported by CNES and CNRS through the GdR MFA. The research of IH was carried out at Jet Propulsion Laboratory, California Institute of Technology, under a contract with NASA.

Data availability The datasets generated during the current study are available from the corresponding author on reasonable request.

Declarations

Conflict of interest The authors declare no Conflict of interest.

References

1. M.S. Green, M. Vicentini-Missoni, J.M.H. Levelt-Sengers, Scaling-law equation of state for gases in the critical region. *Phys. Rev. Lett.* **18**, 1113–1117 (1967). <https://doi.org/10.1103/physrevlett.18.1113>
2. C. Lecoutre, R. Guillaument, S. Marre, Y. Garrabos, D. Beysens, I. Hahn, Weightless experiments to probe universality of fluid critical behavior. *Phys. Rev. E* **91**, 060101 (2015). <https://doi.org/10.1103/physreve.91.060101>
3. M.A. Anisimov, J.V. Sengers, *Critical Region* (Elsevier, Amsterdam, 2000), pp.381–434
4. J. Zinn-Justin, *Quantum Field Theory and Critical Phenomena*, 4th edn. (Clarendon Press, Oxford, 2002), p.1054
5. M. Barmatz, I. Hahn, F. Zhong, M.A. Anisimov, V.A. Agayan, Crossover analyses of heat capacity and susceptibility measurements near the ^3He liquid-gas critical point. *J. Low Temp. Phys.* **121**, 633–642 (2000). <https://doi.org/10.1023/a:1017527930590>
6. I. Hahn, F. Zhong, M. Barmatz, R. Haussmann, J. Rudnick, Crossover behavior in the isothermal susceptibility near the ^3He critical point. *Phys. Rev. E* **63**, 055104 (2001). <https://doi.org/10.1103/physreve.63.055104>
7. C. Bagnuls, C. Bervillier, Classical-to-critical crossovers from field theory. *Phys. Rev. E* **65**, 066132 (2002). <https://doi.org/10.1103/physreve.65.066132>
8. V. Dohm, Nonuniversal critical phenomena along the lambda line of ^4He . *Z. Phys. B* **60**, 61–71 (1985). <https://doi.org/10.1007/bf01312644>

9. R. Schloms, V. Dohm, Renormalization-group functions and nonuniversal critical behaviour. *Europhys. Lett.* **3**, 413–418 (1987). <https://doi.org/10.1209/0295-5075/3/4/005>
10. R. Schloms, V. Dohm, Minimal renormalization without ϵ -expansion: critical behavior in three dimensions. *Nucl. Phys. B* **328**, 639–663 (1989). [https://doi.org/10.1016/0550-3213\(89\)90223-x](https://doi.org/10.1016/0550-3213(89)90223-x)
11. R. Schloms, V. Dohm, Minimal renormalization without ϵ expansion: Critical behavior above and below t_c . *Phys. Rev. B* **42**, 6142–6152 (1990). <https://doi.org/10.1103/physrevb.42.6142>
12. S.A. Larin, M. Mönnigmann, M. Strösser, V. Dohm, Five-loop additive renormalization in the ϕ^4 theory and amplitude functions of the minimally renormalized specific heat in three dimensions. *Phys. Rev. B* **58**, 3394–3408 (1998). <https://doi.org/10.1103/physrevb.58.3394>
13. C. Bagnuls, C. Bervillier, Nonasymptotic critical behaviour from field theory for ising like systems in the homogeneous phase : theoretical framework. *J. Phys. Lett.* **45**, 95–100 (1984). <https://doi.org/10.1051/jphyslet:0198400450309500>
14. C. Bagnuls, C. Bervillier, Y. Garrabos, Experimental data analysis on xenon above the critical temperature from nonlinear renormalization group. *J. Phys. Lett.* **45**, 127–132 (1984). <https://doi.org/10.1051/jphyslet:01984004503012700>
15. C. Bagnuls, C. Bervillier, Nonasymptotic critical behavior from field theory at $d = 3$: the disordered-phase case. *Phys. Rev. B* **32**, 7209–7231 (1985). <https://doi.org/10.1103/physrevb.32.7209>
16. C. Bagnuls, C. Bervillier, D.I. Meiron, B.G. Nickel, Nonasymptotic critical behavior from field theory at $d = 3$. II. The ordered-phase case. *Phys. Rev. B* **35**, 3585–3607 (1987). <https://doi.org/10.1103/physrevb.35.3585>
17. Y. Garrabos, C. Bervillier, Mean crossover functions for uniaxial three-dimensional ising-like systems. *Phys. Rev. E* **74**, 021113 (2006). <https://doi.org/10.1103/physreve.74.021113>
18. Y. Garrabos, C. Lecoutre, S. Marre, R. Guillaument, D. Beysens, I. Hahn, Crossover equation of state models applied to the critical behavior of xenon. *J. Stat. Phys.* **158**, 1379–1412 (2015). <https://doi.org/10.1007/s10955-014-1157-x>
19. F. Zhong, M. Barmatz, I. Hahn, Application of minimal subtraction renormalization to crossover behavior near the ^3He liquid-vapor critical point. *Phys. Rev. E* **67**, 021106 (2003). <https://doi.org/10.1103/physreve.67.021106>
20. F. Zhong, M. Barmatz, Comparison of theoretical models of crossover behavior near the ^3He liquid-vapor critical point. *Phys. Rev. E* **70**, 066105 (2004). <https://doi.org/10.1103/physreve.70.066105>
21. Y. Garrabos, C. Lecoutre, S. Marre, D. Beysens, I. Hahn, Liquid-vapor rectilinear diameter revisited. *Phys. Rev. E* **97**, 020101 (2018). <https://doi.org/10.1103/physreve.97.020101>
22. Y. Garrabos, C. Lecoutre, S. Marre, B. LeNeindre, Critical crossover functions for simple fluids: Non-analytical scaling determination of the ising-like crossover parameter. *J. Stat. Phys.* **164**, 575–615 (2016). <https://doi.org/10.1007/s10955-016-1554-4>
23. V.A. Agayan, Crossover critical phenomena in simple and complex fluids. PhD thesis, Institute for Physical Science and Technology, University of Maryland (2000)
24. V.A. Agayan, M.A. Anisimov, J.V. Sengers, Crossover parametric equation of state for ising-like systems. *Phys. Rev. E* **64**, 026125 (2001). <https://doi.org/10.1103/physreve.64.026125>
25. Z.Y. Chen, P.C. Albright, J.V. Sengers, Crossover from singular critical to regular classical thermodynamic behavior of fluids. *Phys. Rev. A* **41**, 3161–3177 (1990). <https://doi.org/10.1103/physreva.41.3161>
26. Z.Y. Chen, A. Abbaci, S. Tang, J.V. Sengers, Global thermodynamic behavior of fluids in the critical region. *Phys. Rev. A* **42**, 4470–4484 (1990). <https://doi.org/10.1103/physreva.42.4470>
27. J.F. Nicoll, J.K. Bhattacharjee, Crossover functions by renormalization-group matching: $o(\epsilon^2)$ results. *Phys. Rev. B* **23**, 389–401 (1981). <https://doi.org/10.1103/physrevb.23.389>
28. J.F. Nicoll, P.C. Albright, Crossover functions by renormalization-group matching: three-loop results. *Phys. Rev. B* **31**, 4576–4589 (1985). <https://doi.org/10.1103/physrevb.31.4576>
29. F.J. Wegner, Corrections to scaling laws. *Phys. Rev. B* **5**, 4529–4536 (1972). <https://doi.org/10.1103/physrevb.5.4529>
30. M.E. Fisher, P.J. Upton, Fluid interface tensions near critical end points. *Phys. Rev. Lett.* **65**, 3405–3408 (1990). <https://doi.org/10.1103/physrevlett.65.3405>
31. M.E. Fisher, S.-Y. Zinn, The shape of the van der waals loop and universal critical amplitude ratios. *J. Phys. A* **31**, 629–635 (1998). <https://doi.org/10.1088/0305-4470/31/37/002>
32. M.E. Fisher, S.-Y. Zinn, P.J. Upton, Trigonometric models for scaling behavior near criticality. *Phys. Rev. B* **59**, 14533–14545 (1999). <https://doi.org/10.1103/physrevb.59.14533>
33. Y. Garrabos, C. Lecoutre, F. Palencia, B. LeNeindre, C. Erkey, Master crossover functions for one-component fluids. *Phys. Rev. E* **77**, 021116 (2008). <https://doi.org/10.1103/physreve.77.021116>

34. Y. Garrabos, C. Lecoutre, S. Marre, B. LeNeindre, I. Hahn, Critical crossover functions for simple fluids: towards the crossover modelling uniqueness. *J. Stat. Phys.* **165**, 471–506 (2016). <https://doi.org/10.1007/s10955-016-1627-4>
35. Y. Garrabos, Nota.: The fluid-dependent scale parameter was initially noted ϑ in Ref. [14]. In the present work, the notation ϑ_f avoids a possible confusion with the angular variable of CPM noted θ
36. Y. Garrabos, F. Palencia, C. Lecoutre, C. Erkey, B. LeNeindre, Master singular behavior from correlation length measurements for seven one-component fluids near their gas-liquid critical point. *Phys. Rev. E* **73**, 026125 (2006). <https://doi.org/10.1103/physreve.73.026125>
37. Y. Garrabos, B. LeNeindre, R. Wunenburger, C. Lecoutre-Chabot, D. Beysens, Universal scaling form of the equation of state of a critical pure fluid. *Int. J. Thermophys.* **23**, 997–1011 (2002). <https://doi.org/10.1023/a:1016333918357>
38. Y. Garrabos, Is the entropy at the liquid-gas critical point of pure fluids proportional to a master dimensionless constant ? arXiv (2006). <https://doi.org/10.48550/ARXIV.COND-MAT/0601088> . <https://arxiv.org/abs/cond-mat/0601088v1>
39. Y.C. Kim, M.E. Fisher, G. Orkoulas, Asymmetric fluid criticality. i. scaling with pressure mixing. *Phys. Rev. E* **67**, 061506 (2003). <https://doi.org/10.1103/physreve.67.061506>
40. Y. Garrabos, Erratum for Tables I and II of Ref. [17], the notations $X_{p,i}^{+,-}$ on lines 8, 10, and 12, column 2, can be changed to $Y_{p,i}^{+,-}$, with $i = \{1, 3\}$
41. J.S. Kouvel, M.E. Fisher, Detailed magnetic behavior of nickel near its curie point. *Phys. Rev.* **136**, 1626–1632 (1964). <https://doi.org/10.1103/physrev.136.a1626>
42. Y. Garrabos, Facteurs d'échelle phénoménologiques pour la transition critique liquide-gaz des fluides purs. *J. Phys. France* **46**, 281–291 (1985). <https://doi.org/10.1051/jphys:01985004602028100>. see also [cond-mat/0512408](https://doi.org/10.1051/jphys:01985004602028100)
43. Y. Garrabos, Scaling behaviour of the fluid subclass near the liquid-gas critical point. *J. Phys. France* **47**, 197–206 (1986). <https://doi.org/10.1051/jphys:01986004702019700>
44. V. Dohm, Multiparameter universality and intrinsic diversity of critical phenomena in weakly anisotropic systems. *Phys. Rev. E* **108**, 044149 (2023). <https://doi.org/10.1103/PhysRevE.108.044149>